

WEAK INTERACTIONS AT HIGH ENERGIES*

Stanley G. Wojcicki

Stanford Linear Accelerator Center
Stanford University, Stanford, California 94305

(Extracted from the Proceedings of Summer Institute on Particle Physics,
SLAC Report No. 198, November 1976)

* Work supported by the Energy Research and Development Administration.

WEAK INTERACTIONS AT HIGH ENERGIES

Stanley G. Wojcicki

Stanford University
Stanford, California 94305

I. INTRODUCTION

These lectures shall attempt to review the experimental status of high energy weak interactions with a special emphasis on its relation to the physics of "new" particles. In reviewing a field that is moving as rapidly as the high energy neutrino physics today, there is always a difficult choice to be made as to the material to be included. On one hand one can limit oneself to the well established results at the expense of excluding the most recent and hence probably the most interesting data; on the other, one can try to be as all inclusive as possible and thus take the risk of including the results that may already be discredited at the time of publication of the review. I have opted for the latter course and shall try to include all of the data that I am aware of that has been presented publicly, either orally or in written form. It shall fall on the reader to judge the data critically in areas where there is a discrepancy if that discrepancy will not have been resolved already by the time this review appears in print.

I shall commence these lectures with a brief description of the experimental techniques used in high energy neutrino physics with an emphasis on the advantages and limitations of each method. Subsequently, by way of a theoretical introduction, I would like to review the status of the neutrino physics 2 years ago from the point of view of its excellent agreement with the naive quark model. Then, in the main body of these lectures, I would like to discuss the various aspects of the experimental data and see how these results compare with the predictions of the "new orthodoxy" - i.e. the four quark model. Finally, I would like to end by pointing out some of the discrepancies between the theoretical

predictions and the experimental data and comment as to what even newer physics these results might be pointing to.

These lectures shall be limited to the charged current aspect of the neutrino interactions, with the main emphasis on the experimental data. The neutral current data and the deeper theoretical questions are discussed in the parallel lectures by Bjorken.

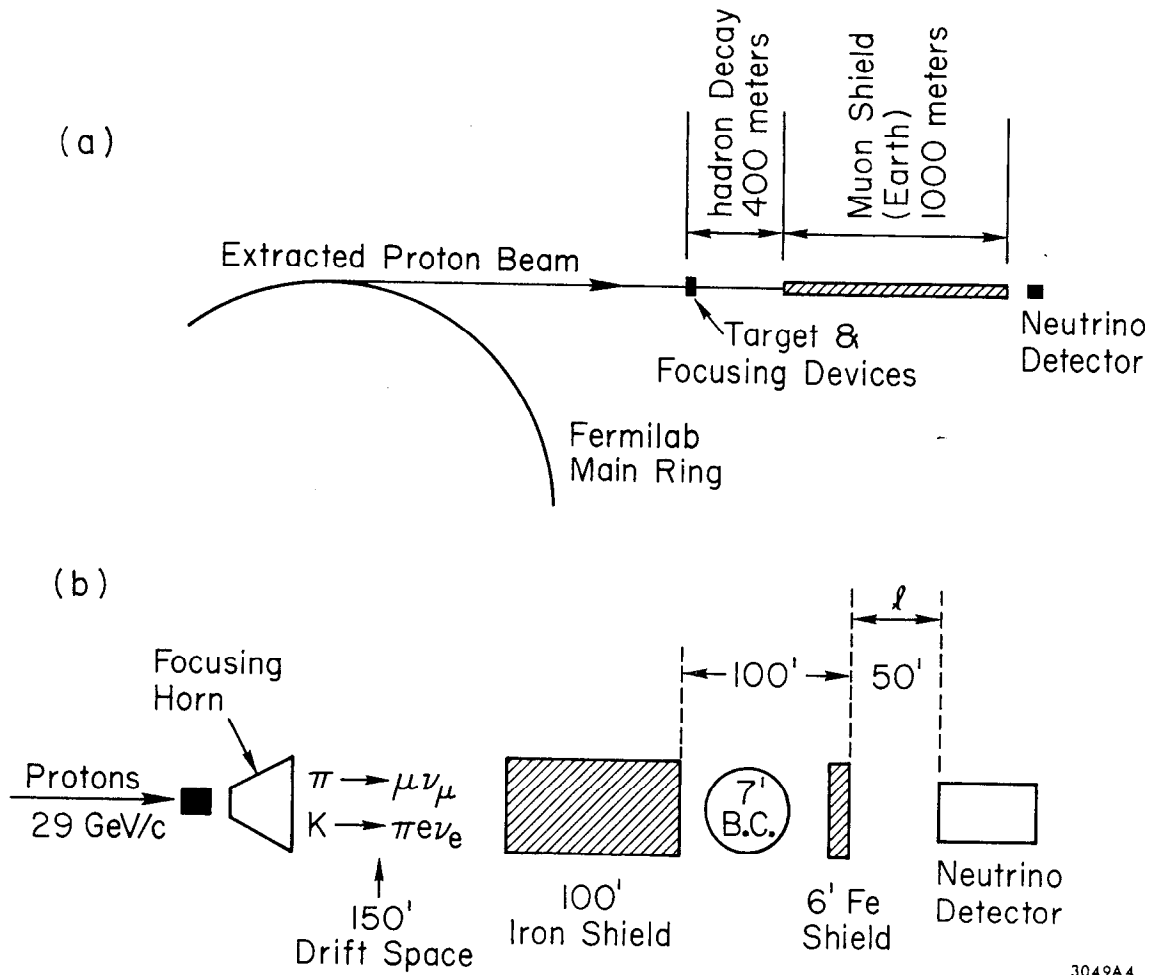
II. EXPERIMENTAL OVERVIEW

a) Beams. All of the high energy neutrino beams used up to this time have utilized the neutrinos originating predominantly from π or K decay. The basic features of all the neutrino beams are illustrated in Fig. 1 where we show schematically the present Fermilab and BNL neutrino setups. The sequential elements of a neutrino beam are:

1. proton beam striking a target and making secondary hadrons.
2. a focusing and/or momentum selecting element(s).
3. drift space, to allow hadrons to decay.
4. a shield to stop all hadrons and range out muons.
5. neutrino detectors.

The most important difference between various neutrino setups resides in points 1, 2 and 5, i.e. incident proton energy, focusing element, and the detector. The length of the drift space and the shield are generally comparable and scale with the energy. The unique feature of all the neutrino setups, illustrated in Fig. 1b, is the ability to stack several detectors one behind the other with only a slight loss of solid angle for the more distant detectors.

A very serious limitation in interpreting the results of a large number of neutrino experiments is the ill defined momentum of the neutrino beam. Accordingly, a great deal of ingenuity has gone into the designs and construction of focusing and momentum selecting elements with the goal of either containing the largest possible number of neutrinos or



3049A4

Fig. 1 A schematic drawing of the Fermilab (a) and the BNL (b) neutrino setups.

purifying and better defining the accepted neutrino flux.

The basic "facts of life" that determine these schemes are the following:

1. the typical transverse momentum of hadrons produced in the hadronic collisions is of the order of 300 MeV/c. This should be compared with 30 MeV/c and 236 MeV/c as the maximum possible p_T that a neutrino can obtain from π and K decay respectively. Thus the hadronic transverse momentum tends to dominate the divergence of the neutrino beam and by focusing the hadrons into a parallel beam one can increase the flux considerably.
2. the present size of the detectors subtends a solid angle at the hadron target comparable to the angular divergence of the highest energy neutrinos. Thus focusing buys relatively little extra flux at high energies and becomes significantly more important for lower energy neutrinos.
3. Because of small $m_\pi - m_\mu$ mass difference the maximum laboratory momentum of a neutrino from π decay is only about 40% of the initial pion momentum. In contrast, a K meson can transfer almost all of its momentum to its daughter neutrino. Thus the highest energy neutrinos come only from K decay. Coupled with the increase of K^+/K^- production ratio as a function of increasing secondary energy, this means that N_{ν^+}/N_{ν^-} ratio will also increase towards the high end of the neutrino momentum spectrum.

In light of these considerations we can now consider various focusing schemes used in neutrino beams.

1. bare target, or absence of any focusing or momentum selecting elements. It is clearly the simplest scheme, but the price paid is low intensity, lack of distinction between ν 's and $\bar{\nu}$'s, and lack of any momentum selection.

2. horn beam. This scheme utilizes a focusing element around the target to focus the hadrons of one sign into a parallel beam. The advantages are maximum possible neutrino (antineutrino) flux and good rejection of the antineutrinos (neutrinos). The disadvantages are short spill (this may actually be an advantage for some experiments, where the desire to gate out the cosmic rays is the most important consideration) and the difficulty in calculating and/or measuring the neutrino flux. The rejection of hadrons of the unwanted sign deteriorates as the energy of the secondaries increases because these particles tend to come out at relatively low angles. This becomes a serious limitation for the study of high energy $\bar{\nu}$ interactions. Accordingly a commonly used variation is a double horn system with a plug down the middle to absorb hadrons produced very close to 0° . This eliminates most of the unwanted ν contamination at the expense of part of high energy $\bar{\nu}$ flux.
3. quadrupole beam. Here the focusing element becomes a quadrupole system set generally to optimize transmission of a relatively high energy hadron beam. This enhances the high energy neutrinos, suppresses the low energy ones, and results in a relatively flat spectrum. The advantages are possibility of a long spill, relative enhancement of higher energy portion of the spectrum, and a relatively good understanding of the neutrino energy spectrum. The disadvantages are lower flux and lack of neutrino/antineutrino selection. The fluxes from all of these schemes are illustrated in Fig. 2, taken from Al Mann's 1976 Coral Gables talk.¹⁾
4. dichromatic beam. Here the beam elements consist of both dipoles and quadrupoles so that the beam entering the decay drift space consists of hadrons with a finite momentum bite and a unique sign. There can be several variations on this idea.

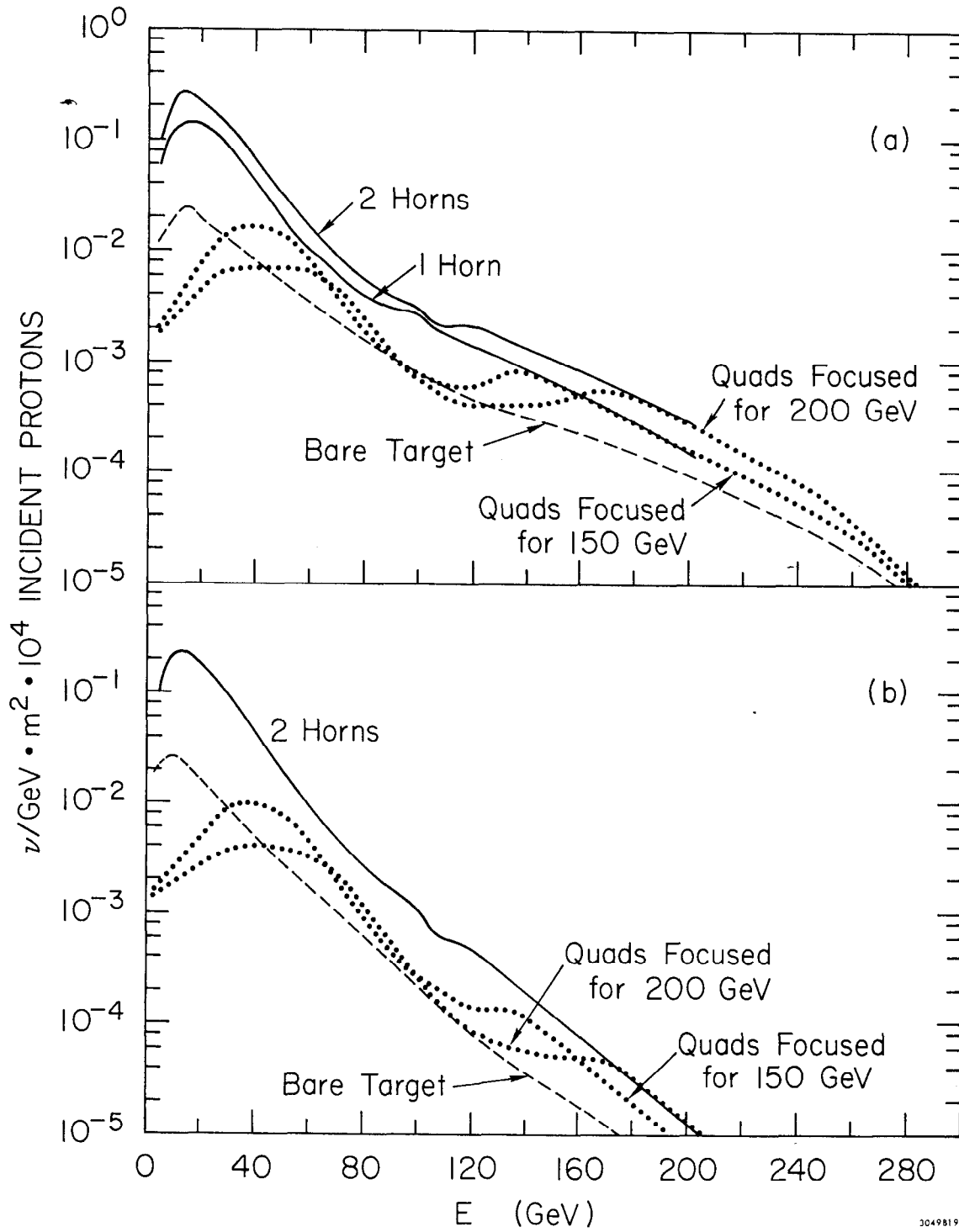


Fig. 2 Calculated neutrino (a) and antineutrino (b) energy spectra for 400 GeV protons.

In the simplest scheme, one utilizes the fact that most of the neutrinos originating from K decay come out at much larger angles than those from π decay.²⁾ Thus a detector of relatively small transverse dimensions will intercept only a small fraction of K neutrinos, or more specifically if positioned at 0° , only the very high energy ones. Hence the spectrum of neutrinos will consist of two discrete bunches, the low energy ones from π decay and the high energy ones from K decay.

A variation of this scheme consists of displacing the detector away from 0° , thus missing the majority of π neutrinos and selecting only the K neutrinos of energy slightly below the peak energy.³⁾ One thus obtains a relatively pure monochromatic neutrino beam. Another variation is making the detector large enough so that a sizable fraction of K neutrinos is intercepted.⁴⁾ The radial position of the interaction is now directly related to the neutrino energy, and one thus has energy information independent of the calorimetry. The basic variations on this dichromatic scheme can be easily seen in Fig. 3, illustrating the K and π decay kinematics.

Clearly the dichromatic beam scheme yields the cleanest neutrino beam. The price that one has to pay, however, is the significant reduction in flux resulting from the finite momentum bite.

b) Detectors. In discussing the detectors used in the neutrino experiments it is convenient to divide them into two categories: the electronic detectors and the bubble chambers. We commence with a brief discussion of the electronic detectors. The typical neutrino apparatus performs the combined functions of a target, hadron detector, and muon spectrometer. The different setups can be classified according to how the various parts of the detector are arranged.

1. separate function detector. Here the target-hadron detector part of the apparatus comes first and is subsequently followed by a magnetic system to analyze the muons. Such a system has

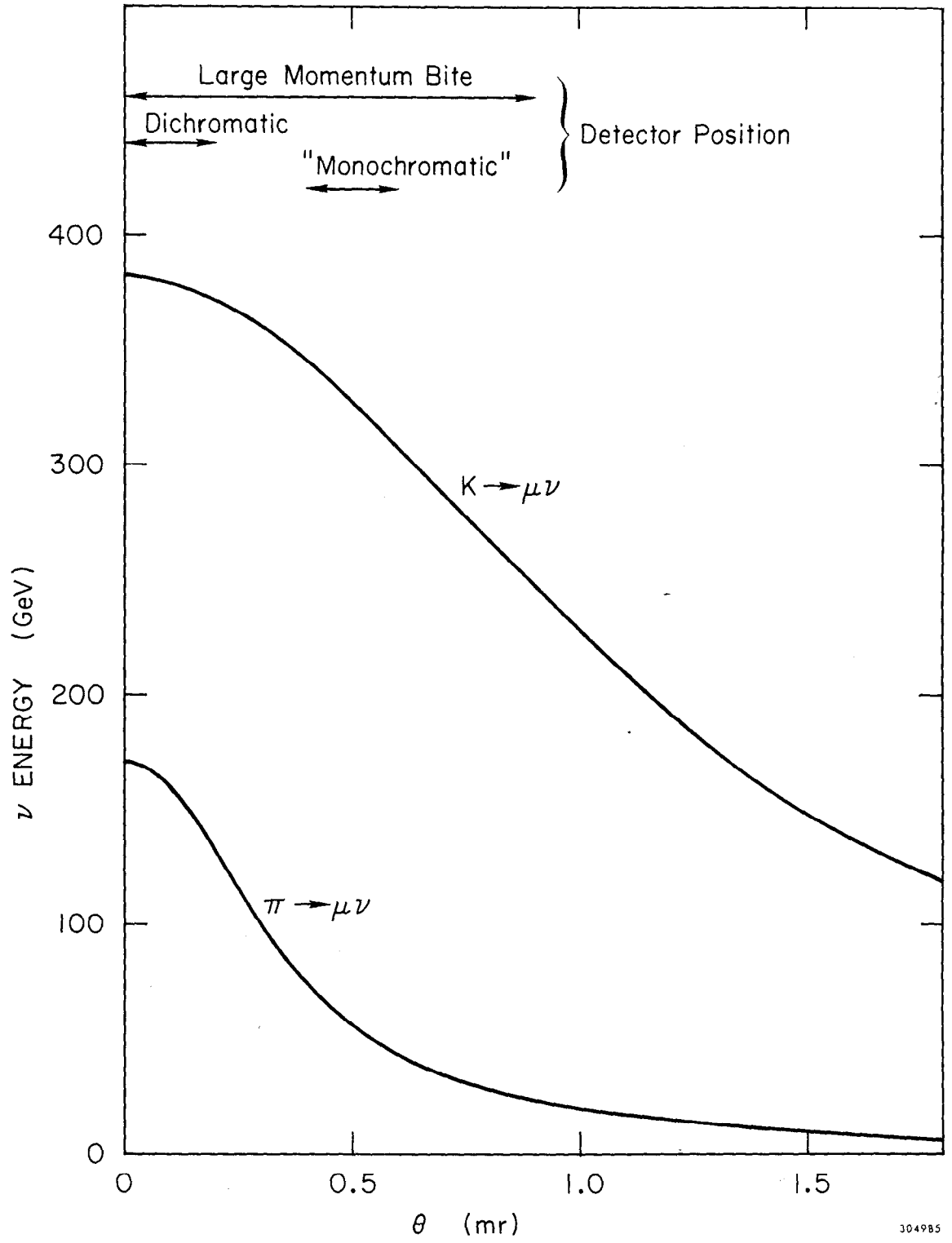


Fig. 3 K and π decay kinematics.

a relatively high flexibility from the point of view of changes in the target part but a relatively poor acceptance, especially for wide angle muons. The Harvard-Penn-Wisconsin-Fermilab (HPWF) setup and the old Cal-Tech-Fermilab setup (E21) fall into this category.

2. combined function detector. The target, hadron detector, and the muon spectrometer are all interleaved together. The system has very high acceptance for muons, but loses some flexibility. The new setup at CERN SPS exemplifies this kind of approach.
3. mixed detector. A separate target-detector is subsequently followed by a combined function detector. The new Cal Tech setup at Fermilab falls into this category.
4. non magnetic detectors. There are also used special purpose detectors without any magnetic field. These have been used for specific experiments at relatively low energies where the large acceptance is more important than magnetic analysis. The 2 setups to measure elastic ν scattering at BNL exemplify this category.

As with all classifications, these should not be considered very rigid, but rather as exemplifying the different ways of arranging the separate parts of the apparatus. Thus, for example, placing a hydrogen target in front of the CERN SPS detector would turn it into a mixed detector in our nomenclature.

The bubble chamber systems can be classified into two categories: cryogenic and warm chambers. The cryogenic chambers use hydrogen, deuterium, or neon as the fill or some combination of these ingredients. The obvious advantage of hydrogen or deuterium is the simplicity of the target; the obvious disadvantages: low target mass, long absorption length (~ 8 m for H_2) and long radiation length (~ 9 m for H_2). These last two

factors make the lepton identification very difficult and make complimentary electronic detectors highly desirable.

The warm bubble chambers, of which the European Gargamelle is the most famous example, generally use an organic fill with higher density and shorter radiation length than even the neon filled chambers. In that sense they are highly complimentary to the hydrogen chambers, emphasizing good lepton identification with the simultaneous introduction of a complicated target.

c) Energy Measurement. The measurement of the total energy (hadronic, leptonic, and electromagnetic) in neutrino interactions is an important problem as it is crucial both to the cross section and scaling variable measurements. Thus it is worthwhile to briefly point out here the advantages and shortcomings of different beams and/or detectors.

The dichromatic beam, at least in principle, is the ideal instrument to measure the total neutrino energy, as a crude calorimetry measurement of the total hadronic energy in the detector will allow one to separate π and K neutrino interactions. Then, if the momentum bite of the beam is small enough, and the beam clean enough, the energy of the neutrino is defined quite well.

In wide band and quadrupole beams one must rely exclusively on the calorimeter and muon spectrometer to measure the total energy. The typical accuracy here is about $\pm 10\%$. Of course this technique will only give a lower limit if some secondary neutrinos are given off in the interaction.

The "heavy fill" bubble chambers can in principle use visual calorimetry to measure total energy with some correction for the escaping neutrals. The light fill bubble chambers, where most of the neutrals (n , K^0 , γ) escape detection, generally measure total energy present in charged particles and then, using an empirical formula, scale this to the total energy.

d) Lepton Identification. The electron identification is easy only in "high" Z bubble chambers. More specifically, a medium Z fill, like 80% H₂ and 20% Ne, makes the electron identification possible at about 50% efficiency level in the 15' B.C., but the identification requires rather careful scanning. The techniques used here rely on visible bremsstrahlung, e[±] materialization, trident production, and delta rays, as unique signatures of the e[±]. The electron identification in a much heavier fill, like freon in Gargamelle, is quite straightforward, almost 100% efficient, and completely unambiguous. The relative merits of various fills in identifying electrons and muons are illustrated in Table I.

TABLE I

The absorption and radiation lengths for various bubble chamber fills.

	Absorption Length	Radiation Length
Hydrogen	790 cm	890 cm
Deuterium	342 cm	764 cm
"Light" neon-hydrogen (21% Ne)	230 cm	110 cm
Neon	75 cm	24 cm
Propane (C ₃ H ₈)	176 cm	111 cm
Freon (CF ₃ Br)	73.5 cm	11 cm

There have been efforts to identify electrons in electronic detectors,⁵⁾ and they have met with some measure of success. On the other hand the basic incompatibility of the large target mass necessary for neutrino experiments and low graininess required for good electron identification and measurement make these experiments extremely difficult.

On the other hand the electronic detectors find the muon identification considerably easier, with penetration through some 1 kg/cm² of material a relatively clean signature. Of course this technique becomes much more difficult for lower energy ($P_{\mu} < 1.5 \text{ GeV}/c$) muons, since they tend to range out before hadrons can be cleanly eliminated.

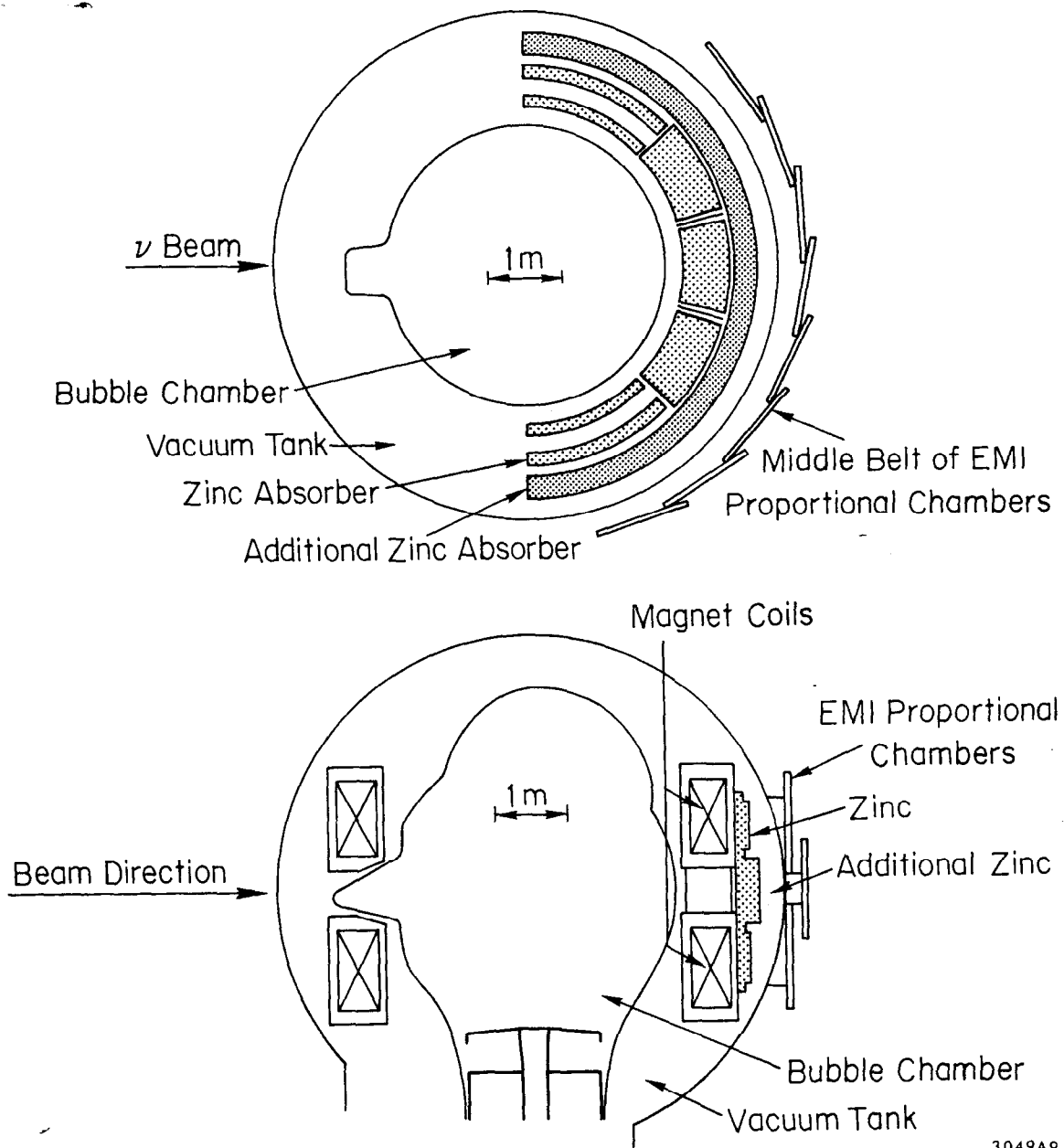
In general, even for heavier fills, the absorption length in bubble chambers is comparable to the potential pathlength in the detector and

thus "bare" bubble chambers suffer in their ability to detect muons. The external muon identifier (EMI) around the 15' chamber⁶⁾ remedies this difficulty by essentially extending the sensitive volume beyond the bubble chamber (see Fig. 4). It consists of a layer of proportional chambers preceded by several absorption lengths of zinc. Requiring a correlation between the B.C. track and a hit in PWC's provides a powerful rejection against hadrons. The main shortcoming of the EMI at the present time is its limited solid angle.

The bubble chamber experiments have been quite successful in using kinematics to identify the muon. Here one relies on the fact that muons tend to have high energy and high Q^2 . Comparison with EMI results indicates that on the average one can do quite well in identifying muons by this technique, but of course the method is ineffective for muons in kinematically suppressed regions.

e) Strange Particle Identification. This facet of experimental detection, very important in the context of new particle production, has been almost an exclusive preserve of the bubble chambers. Heavy fill bubble chambers have some difficulty separating Λ 's from K^0 's. The K^+ 's so far have been identified solely in bubble chambers either by their decays or by stopping. Because of very strong bias toward low energy K 's, and the very low efficiency, charged K identification has not been used so far in any systematic way.

f) Summary of Existing Detectors. It appears worthwhile to end this purely experimental section with a table summarizing the vital statistics of the existing neutrino setups. This list will soon be enlarged by the new CERN-SPS detectors and the new Cal-Tech-Fermilab-Northwestern detector.



3049A9

Fig. 4 The External Muon Identifier for the 15' Fermilab bubble chamber.

TABLE II

Experimental neutrino setups.

Group	Detector	Size/Fid.Size	Laboratory	Proton Energy
	HBC	7'	BNL	30 GeV
	HBC	12'	Argonne	12 GeV
	HBC	15'	Fermilab	400 GeV
	GGM	12'/3m ³	CERN	25 GeV
HPWF	Liquid Sc.	60 tons	Fermilab	400 GeV
CITF	Fe	170 tons	Fermilab	400 GeV
USSR	Fe	96/34 tons	Serbukhov	70 GeV
CIR	Al	26/8 tons	BNL	30 GeV
HPW	Liquid Sc.	33 tons	BNL	30 GeV

III. NEUTRINO PHYSICS AND THE NAIVE QUARK MODEL

We would like to start the discussion of the status of neutrino physics by summarizing the predictions of the naive quark model and show its excellent agreement with what was known 3 years ago. Very briefly the essential features of the simple quark model are the following.

The neutron and proton are each composed of three quarks, namely $2d + u$ and $2u + d$ respectively. The up (u) quark carries a charge of $+2/3$, the down (d) quark a charge of $-1/3$. In addition, there may be a sea of quark-antiquark pairs whose presence would be exhibited mainly at low values of Feynman x . The quarks are point constituents without any form factors and thus lepton nucleon scattering can be treated in terms of superposition of fundamental current - quark interactions. All the weak interactions occur via V-A couplings and thus only the left handed quarks (or right handed sea antiquarks) participate in the reaction. Finally, since the same quarks also are responsible for the deep inelastic e-p scattering, the structure functions, i.e. "momentum" distributions of the quarks in the nucleons, as derived from e-N scattering can be carried over directly to the neutrino interactions.

This simple picture leads right away to several quantitative predictions. Thus, since the fundamental charged current neutrino reaction

can occur only on the down quark, i.e.

$$\nu d \rightarrow u \mu^-$$

the νn to νp cross section ratio should be 2 to 1, a simple consequence of the relative number of the down quarks in the two nucleons. More refined analysis,⁷⁾ incorporating the actual structure functions and the sea quarks, yield predicted ratios of between 1.57 and 2.05 in fair agreement with the experimental numbers of

1.48 ± 0.17	7' BC experiment at BNL ⁸⁾
$1.4 \pm .3$	12' BC experiment at Argonne ⁹⁾
2.1 ± 0.3	Gargamelle experiment ¹⁰⁾

Another simple prediction is the agreement of neutrino derived structure functions with those obtained from the ep scattering. This agreement was first seen in the Gargamelle data¹¹⁾ and is illustrated in Fig. 5. One should emphasize here that the agreement of the absolute normalization constitutes an experimental verification of the mean square charge of the quark in the nucleus being 5/18 as predicted by the quark model. This is because the coupling of the electromagnetic current to the quark is proportional to the electric charge squared, a factor which is absent in the weak current coupling. Alternatively we can look on the size of the neutrino cross section as constituting a measurement of the mean square charge of the quark.

The relative size of the neutrino and antineutrino cross sections also follows directly from the quark model, it being the consequence of the V-A nature of the coupling. If we look at the neutrino quark scattering in the center of mass both 0 and 180° scattering are allowed by the required helicity and the conservation of angular momentum.

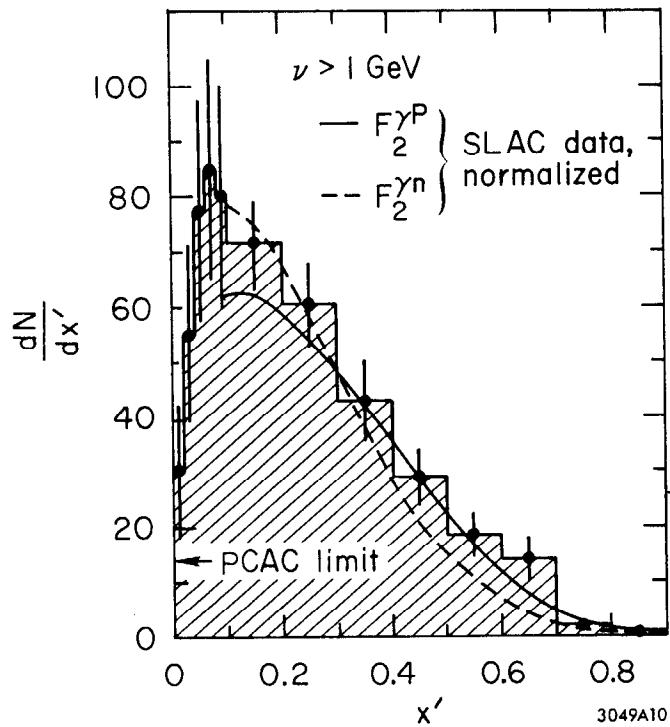
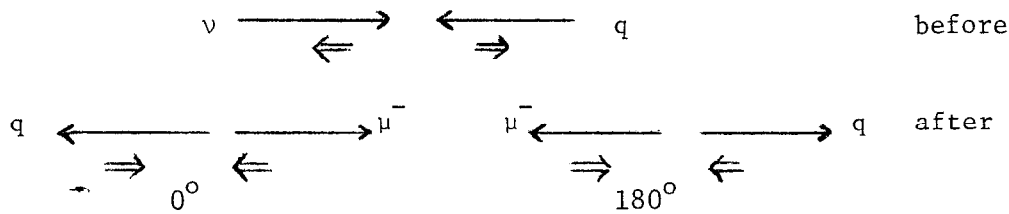
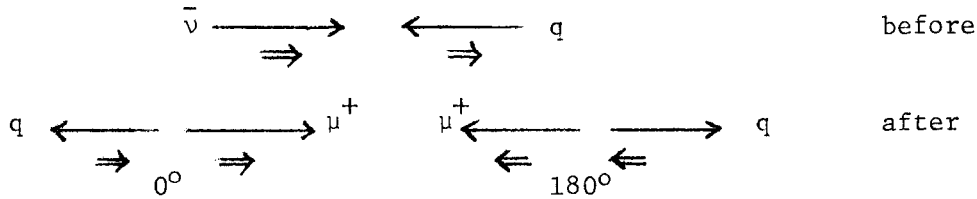


Fig. 5 Comparison of the Gargamelle neutrino data with the structure function obtained from SLAC ep and ed data. Because of low energies the Bloom-Gilman variable x^1 is used rather than x .



However, for antineutrino quark scattering 180° scattering is forbidden by angular momentum conservation, since it is impossible to both conserve



the angular momentum and maintain the proper helicity of the two scattering particles. More quantitatively, in terms of the scaling variable $y \equiv \frac{E_h}{E_\nu}$, the neutrino distribution will be flat and the antineutrino one will follow $(1-y)^2$, giving the required zero at $y = 1$ i.e. 180° scattering in the center of mass system. Integrating we obtain the predicted ratio

$$\frac{\sigma_{\bar{\nu}}^{\text{TOT}}}{\sigma_{\nu}^{\text{TOT}}} = 1/3$$

to be compared with the original experimental results of

	0.38 ± 0.04	1-10 GeV	GGM	12)
	0.40 ± 0.11	38 GeV	CIT-F	13)
	0.23 ± 0.11	110 GeV	CIT-F	13)
and	0.34 ± 0.03	10-30 GeV	HPWF	14)

Similarly the original "low energy" (i.e. $E_{\nu, \bar{\nu}} \leq 30$ GeV) data appeared to reproduce the predicted $d\sigma/dy$ distributions for both the ν and $\bar{\nu}$ scattering.

Finally, the total cross section for ν and $\bar{\nu}$ interactions should follow a linear behavior with E , a consequence of point nature of the neutrino quark scattering. The agreement with the data as of two years ago was indeed excellent as can be seen in Fig. 6.

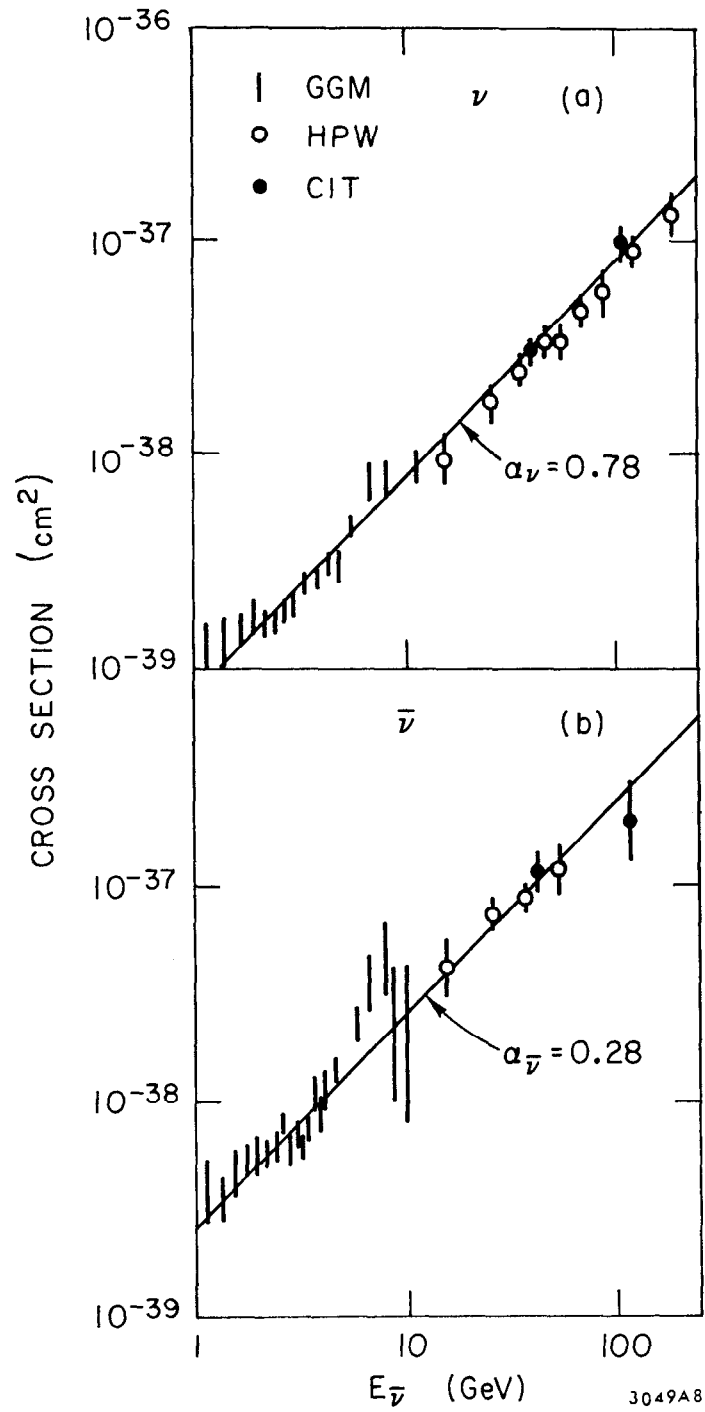


Fig. 6 Early measurements of total ν and $\bar{\nu}$ cross sections as a function of energy (from 1974 London Conference).

In summary, even though the detailed predictions of the model were not tested rigorously, the low energy neutrino data appeared to be in very good agreement with the predictions of the simplest quark model.

IV. 4 QUARK MODEL PREDICTIONS

We consider next the ramifications of the 4 quark model on the neutrino physics. In this picture the hadronic current becomes

$$J_{\mu}^{cm} = \bar{u} \gamma_{\mu} (1-\gamma_5) d_c + \bar{c} \gamma_{\mu} (1-\gamma_5) s_c$$

where $d_c = d \cos \theta_c + s \sin \theta_c$

$$s_c = -d \sin \theta_c + s \cos \theta_c$$

and the s and c are the strange and charmed quark respectively and θ_c is the Cabibbo angle.

We must remember now that the Cabibbo angle is small, i.e. $\sin^2 \theta_c \approx 0.05$ and that the number of s and c quarks and antiquarks in the nucleons is supposed to be small, since their only source is the sea of quark-antiquark pairs that should be important only at low x. It is for these two reasons that the naive 2 quark model can be expected to give good results even if the 4 quark picture represents the "ultimate truth". This is especially true at low energies where the charmed quark production is negligible or even below threshold.

We may now consider specific mechanisms that can lead to charmed particle production in neutrino interactions.

a) $\underline{\nu d \rightarrow \mu^- c}$. This process would be suppressed by $\sin^2 \theta_c$ with respect to other charged current reactions. Furthermore, the equivalent process involving the valence quarks does not exist for the $\bar{\nu}$'s.

b) $\underline{\nu s \rightarrow \mu^- c}$
 $\underline{\bar{\nu} \bar{s} \rightarrow \mu^+ \bar{c}}$

This process must proceed off sea quarks. Thus it should be dominant at low x and the general level should be $\sim 5-10\%$ (i.e. fraction of sea

quarks indicated by low energy neutrino experiments).

- c) $\bar{\nu}_c \rightarrow \mu^- \bar{s}$ c quark is "liberated"
 $\bar{\nu}_c \rightarrow \mu^+ s$ \bar{c} quark is "liberated"

This process should be suppressed even more than (b) as the $c\bar{c}$ sea is expected to be even smaller than the $s\bar{s}$ sea due to the higher mass of the charmed quark.

d) Diffraction Production of F^* . F^* is expected to have the same quantum numbers as the weak current and thus the weak current could transform directly¹⁵⁾ in the presence of a nucleon into F^* . However, because of observed low production of ρ mesons in the neutrino interactions, which can also proceed via this mechanism, this process is expected to be relatively unimportant.

We can now turn to the question of the signatures of the charmed particle production in neutrino interactions.

a) Bumps in the Hadronic States. These would have to have specific features in order to be associated with charm particles:

Narrow - i.e. consistent with resolution, since the charmed ground states would decay via weak interactions.

Massive - the mass would be expected to be around 2 GeV.

Strange - the predominant decay modes could be expected to involve strange particle decay.

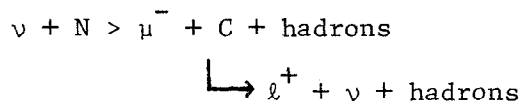
Exotic - the charge and strangeness quantum numbers of the parent state would be expected to have opposite sign.

This is certainly a classical way to look for new short lived particles. For several reasons, however, it is difficult as far as charmed particles are concerned. Firstly, at the present time it is accessible only to the bubble chambers and thus the numbers of events are rather limited. Secondly, the many expected decay modes require large statistics to obtain a meaningful signal. Finally, one expects large multiplicity because of

high mass, and this makes the detection of neutral particles very important. Low Z chambers have good resolution but poor detection probability; the high Z chambers have much better detection efficiency but much worse resolution.

The present statistics of bubble chambers are too limited to offer any substantial contribution here, but one can expect significant increase in the data in the next few years.

b) Di-lepton Production. The charmed particle production can give rise to dilepton production via the mechanism



where C is some charmed meson or baryon. This mechanism would yield dileptons of opposite sign because of the $\Delta Q/\Delta C$ rule which is operative here both in the production and the decay processes. Some additional features associated with this process which would lend further credence to charmed particle production interpretation are associated strange particle production, asymmetry between μ^- and μ^+ , i.e. mostly $P_{\mu^-} > P_{\mu^+}$, and relatively high P_T of μ^+ .

c) $\Delta Q/\Delta S$ Violation. There is by now very good evidence from low energy weak decay processes that $\Delta Q/\Delta S$ rule holds down to the level of a percent or so in amplitude. The combined production and decay process of a charmed particle in neutrino interactions is expected to yield $\Delta Q = -\Delta S$ since the production process would have $\Delta Q = +1$ and $\Delta C = +1$ and the decay process $\Delta C = -1$ and $\Delta S = -1$. Thus observation of a reaction with $\Delta Q = -\Delta S$ would be strong evidence for charmed particle production. Unfortunately, to be convincing, any purported evidence for $\Delta Q = -\Delta S$ must be able to exclude associated production, i.e. other missing strange particles. These could be charged K's misidentified as π 's or escaping K_L^0 's. Thus this technique must demonstrate the absence of missing K's either on

a statistical basis, necessitating good statistics, or on an individual basis by means of a highly constrained fit. The latter situation would strongly favor low energy where, however, the charm production is expected to be smaller. It is doubtful that any other detector besides bubble chambers would be able to demonstrate $\Delta Q/\Delta S$ rule violation.

d) Strange Particle Excess. From the production mechanisms discussed above, and the fact that charmed particles should decay predominantly into strange particles, we can anticipate one or two strange particles in the final state for every charm event. Thus one might expect a rise in strange particle yield well above charm production threshold.

e) Anomalies in Scaling Variables. Charm production would represent an onset of new phenomena and thus would imply that there is a relevant mass scale of the order of few GeV. Thus we would expect a change in scaling variable behavior when we pass the charm threshold. Most specifically, for kinematical reasons, the effects of new particles soon after threshold would exhibit themselves as enhancements at low x , high y , and high W .

In conclusion, one should point out that at least some of these manifestations, e.g. dilepton production and scaling variable anomalies, are not specific to the charm model, but would apply equally well to any new particle production with new quantum number. What distinguishes the charmed particle model from other possibilities is the specific nature of its predictions. It not only makes additional predictions regarding strange particle excess, but it also sets at least approximately the level at which charmed particle production may be expected. This level is relatively small due both to the smallness of the Cabibbo angle and the fact that the sea contribution, as measured by the initial neutrino experiments, is relatively small (i.e. at the 5-10% level).

V. EXPERIMENTAL STATUS OF DILEPTONS

a) Experimental picture of μe Events. The initial μe events produced by neutrinos were observed in the Gargamelle exposure at CERN¹⁶⁾. Because of the very short radiation length, the electron identification is unambiguous as can be seen from one of the events displayed in Fig. 7. The main background comes from asymmetric e^\pm pairs, resulting either from Dalitz or external conversion of γ rays. On the basis of analysis of 44.5 K charged current events with visible energy greater than 1 GeV one can reach several conclusions.¹⁷⁾

1. $\mu^- e^+ V^0$ events are seen. 3 clear examples have been observed, in two of which the V^0 is ambiguous in its interpretation between K^0 and Λ . In the third event the V^0 is definitely a Λ . In addition a fourth event has a neutron star and 2 external e^\pm conversions but no V^0 . Thus it is a strong candidate for a $\Lambda \rightarrow n\pi^0$ decay. The expected $\mu^- e^+ V^0$ background is less than 0.1 event.
2. $\mu^- e^+$ events without a V^0 have also been seen.
3. there is a strong correlation between the observation of a $\mu^- e^+$ event and presence of a V^0 . If they were uncorrelated, one would expect 256 (rather than 16 observed) $\mu^- e^+$ events based on 3 seen $\mu^- e^+ V^0$ events.
4. there were no $\mu^+ e^- V^0$ events seen in $\bar{\nu}$ events (in a sample about 1/5 as big).
5. the authors do not quote a rate for this process but an estimate can be obtained from previously published upper limit on charmed particle production (Fig. 8) based on a sample of 6.1K charged current events and 1 observed $\mu^- e^+ V^0$ event. Assuming the same neutrino spectrum, we get for production cross section by neutrinos above 3 GeV

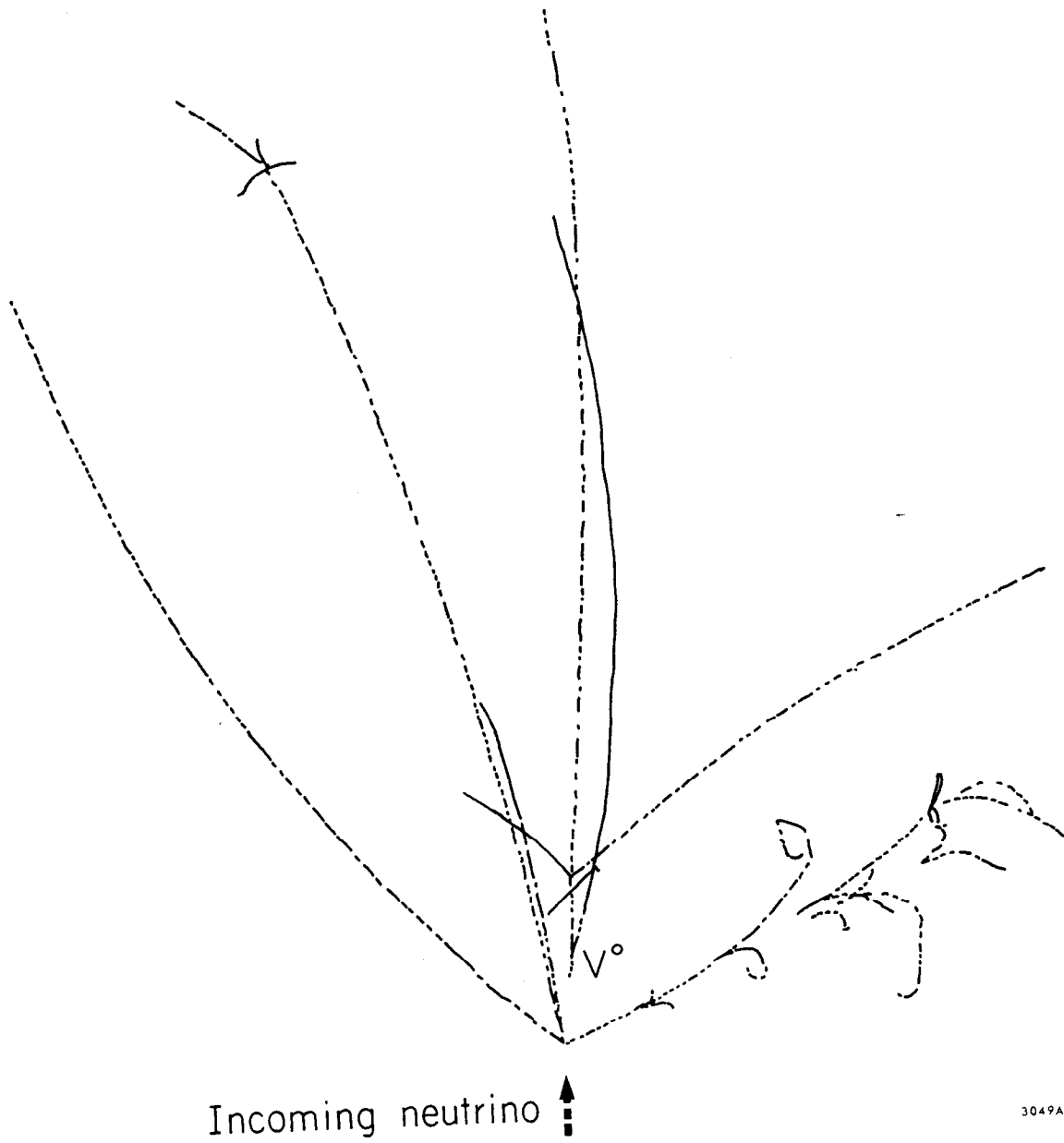


Fig. 7 An example of one of the $3 \mu\text{eV}^0$ events seen in the Gargamelle.

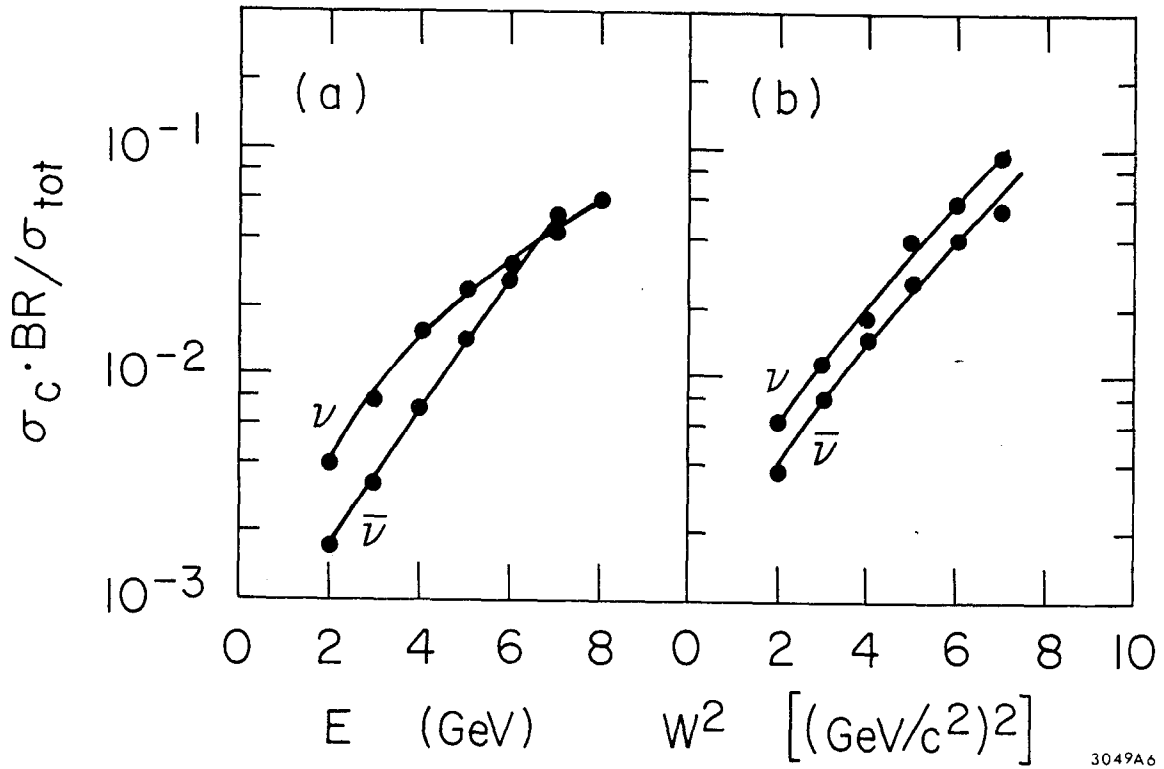


Fig. 8 The initially published Gargamelle upper limits for charmed particle production followed by its decay into a $\mu e \nu^0$.

$$\frac{\sigma_c \cdot \text{BR}}{\sigma_{\text{TOT}}} = 8 \times 10^{-3} \times \frac{1}{2.3} \times \frac{6.1}{44.5} \times 3 \approx 1.5 \times 10^{-3}$$

The results on the μe search of the Gargamelle Collaboration are summarized in Table III.

TABLE III

Observed and expected (from background sources) numbers of μe events.

Event Type	Numbers of Events	
	Observed	Expected
$\mu^- e^+ \nu^0 + \text{anything}$	3 ^(±)	$\sim 9 \times 10^{-2}$ (±)
$\mu^- e^+ + \text{anything}$	16	5 ± 3
$\mu^- e^- + \text{anything}$	23	25.6 ± 8.0
$e^- \nu^0 + \text{anything}$	5	2.5 ± 0.8
$e^+ + \text{anything}$	6	5.4 ± 1.6

(±) These numbers refer to the full experiment (44500 CC events above 1 GeV) whilst the remaining numbers refer to the 1975 run (34100 CC events above 1 GeV).

The Columbia-BNL group has tried to extract information on μe production from their experiment designed to study neutrino nucleon elastic scattering using an array consisting of Al spark chambers and scintillators.¹⁸⁾ The muon identification is straightforward, but the electron identification is very difficult, the main backgrounds being γ ray conversions near the interaction vertex and ν_e interactions (about 1% of events.) The μe events are isolated by requiring the first spark of the "electron" track to be close to the vertex and a reasonable length of straight track before shower initiation.

The authors claim observation of 7 events, of which at least 4 they believe to be genuine $\mu^- e^+$ events. They quote the rate for observed events

$$\frac{\mu e}{\text{ALL}} \approx 3 \times 10^{-4}$$

On the other hand, one must remember that the cuts are very severe, so that if the analysis is correct the actual rate must be considerably higher.

Recently the Wisconsin-Berkeley-CERN-Hawaii group¹⁹⁾ presented the first results from the exposure of Fermilab 15' bubble chamber filled with a light Ne-H₂ mixture to a wide band horn focused neutrino beam. The 20% Ne mixture shortens the radiation length to 110 cm and thus allows one to identify approximately 50% of the electrons above 800 MeV by looking for accompanying tridents, conversion pairs, or sudden changes in curvature (bremstrahlung). By following the identical procedure on converted γ rays the actual conversion efficiency has been measured to be $48 \pm 7\%$ and essentially flat for electrons above 800 MeV. The collaboration draws several conclusions based on a scan of some 5000 ν interactions with the total observed energy above 5 GeV.

1. 15 $\mu^- e^+$ events have been observed.
2. There is a strong correlation between those events and the presence of a strange particle. More specifically, one sees in association 7 K^0 's, 2 Λ 's, and 2 V 's ambiguous between K^0 and Λ . Furthermore 2 K^+ 's are identified unambiguously. This should be compared with 16% of all charged current events at this energy being associated with a V^0 .²⁰⁾
3. The observed number of K^0 's, after correcting for neutral and K_L^0 decays yields the average number of K^0 's/event $\langle N_{K^0} \rangle = 2.0 \pm 0.6$.
4. There is a strong asymmetry between μ^- and e^+ , with

$$\frac{\langle P_{\mu^-} \rangle}{\langle P_{e^+} \rangle} = 6.6$$

5. There is no evidence for any apparent production threshold, with a possible hint of cross section dropping somewhat below 20 GeV.
6. The production rate depends on the specific model assumed for charmed particle production and decay, since the experiment is sensitive only to electrons above 800 MeV. Taking

Barger's and Phillip's model²¹⁾ of $D \rightarrow K e \nu$ decay, one obtains

$$\frac{e^+ \mu^-}{\text{ALL}} \approx (1 \pm 0.3) \times 10^{-2}$$

The same fill of the bubble chamber was also exposed to the wide band horn $\bar{\nu}$ beam by the FNAL-IHEP-ITEP-Michigan collaboration.²²⁾ Out of a total of 644 events with energy greater than 10 GeV they find one rather poor candidate, with $E_{\bar{\nu}} = 36$ GeV, where a background of 0.4 ± 0.2 events is expected. The upper limits on the total new particle production rate times the branching ratio into $\mu e (V^0)$ are given as the function of energy in the accompanying table.

TABLE IV

Upper limits on e production by antineutrinos.

$E_{\bar{\nu}}$ *)	μ^+ Events	$\sigma(\mu^+ e^-) / \sigma(\mu^+ s)$	$\sigma(\mu^+ e^- V^0) / \sigma(\mu^+ x)$
>10 GeV	644	$\leq 1.0\%$	$\leq 0.6\%$
>20 GeV	366	$\leq 1.7\%$	$\leq 1.0\%$
>30 GeV	191	$\leq 3.2\%$	$\leq 1.9\%$
>40 GeV	88	$\leq 4.1\%$	$\leq 4.1\%$

*) An average correction for neutral energy loss has been applied.

b. Review of the $\mu^+ \mu^-$ Situation. The first 2 $\mu^+ \mu^-$ events produced in neutrino interactions have been observed by the HPWF group some 3 years ago and reported at the London conference.²³⁾ Since that time the group has considerably extended this investigation²⁴⁾ by greatly increasing the statistics, studying the phenomenon with several different beams, and doing a more detailed analysis of all the relevant variables. The muons are required to penetrate through sufficient steel so as to unambiguously eliminate the possibility of hadron punchthrough. This does, however, set a lower limit on the detectable muon momentum of 4 GeV/c.

The main conclusions reached by the HPWF group are the following.

1. the events definitely do not come from π and/or K decay and thus must represent new physics. The basic justification for this statement comes from the fact that the production ratio in light (liquid scintillator) and heavy (iron) target are the same. Those two targets differ in their mean density by a factor of 3.54. To take into account the slightly different detection efficiencies for the two targets a Monte Carlo calculation was performed yielding the result that π -K decay process can be excluded as the sole source of $\mu^+\mu^-$ events at the 4σ level. These results are presented graphically in Fig. 9.
2. The visible energy is high but the ratio of $\mu^+\mu^-$ events to all the charged current events is constant above about 40 GeV.

More specifically one obtains

$$\frac{\mu^+\mu^-}{\mu^-} = (0.8 \pm 0.3) \times 10^{-2} \text{ at } \bar{E}_\nu = 100 \text{ GeV based on 51 } \mu^+\mu^- \text{ events}$$

and

$$\frac{\mu^+\mu^-}{\mu^-} = (0.9 \pm 0.3) \times 10^{-2} \text{ at } \bar{E}_\nu = 55 \text{ GeV based on 14 } \mu^+\mu^- \text{ events}$$

The large neutrino energy responsible for these events is illustrated in Fig. 10 where for comparison we also plot the energies of the first 7 μ^-e^+ events observed in the 15" B.C. and the calculated ν spectrum for the conditions under which these $\mu^+\mu^-$ data were taken. One should be very careful, however, about drawing any conclusions about threshold from these data since there is a strong bias against detection of lower energy neutrino events. Without a specific production and decay model it is impossible to estimate the actual magnitude of this bias. Furthermore, one must remember that the μ^-e^+ events have quite different biases and were taken in a horn beam that strongly emphasizes lower energy neutrinos (c.f. Fig. 2a).

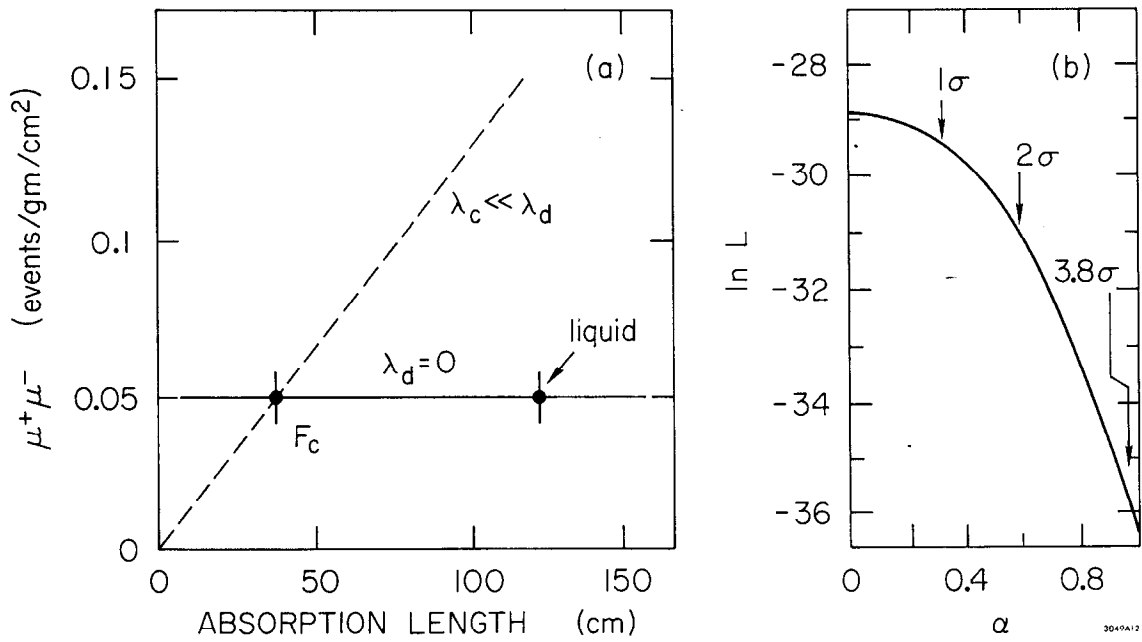


Fig. 9 a) the number of $\mu^+\mu^-$ events g cm^2 as a function of the absorption length. b) results of the likelihood analysis of the fraction α of events that arise from π or K decays.

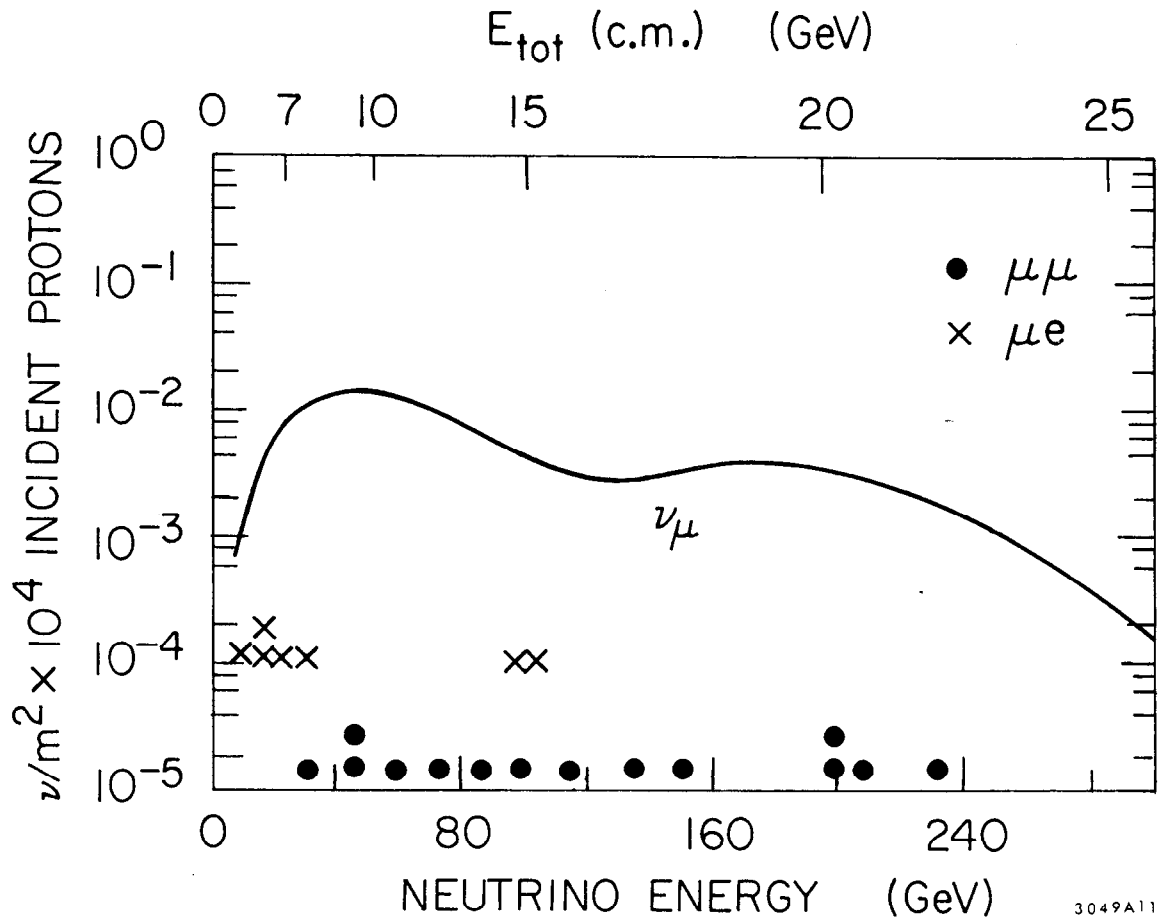


Fig. 10 Total energy distribution of the $\mu^+\mu^-$ events and of the μ^-e^+ events.

3049A11

3. there is a strong asymmetry between μ^- and μ^+ with ratio for all events being

$$\frac{\langle p_- \rangle}{\langle p_+ \rangle} = 3.7 \pm 0.65.$$

Some fraction of these events are most likely caused by the antineutrinos since the data were taken in a quadrupole focused beam. Thus if one makes the assumption that the higher energy muon carries the lepton number of the incoming neutrino, then one can remove the 9 events with $P_- < P_+$ on the assumption that these are produced by $\bar{\nu}$. One then obtains for the ratio

$$\frac{\langle P_- \rangle}{\langle P_+ \rangle} = 6.1 \pm 0.8$$

The support for the validity of this assumption is provided by the independent run²⁵⁾ with a double horn $\bar{\nu}$ beam which yielded 5 $\mu^+ \mu^-$ events, 4 of which had $P_+ > P_-$. This is quite significant since $\bar{\nu}/\nu$ ratio in that beam is of the order of 10. For the $\bar{\nu}$ horn run one obtains the rate ratio of

$$\frac{\mu^+ \mu^-}{\mu^+} = (2 \pm 1) \times 10^{-2}$$

i.e. consistent with the ν data.

4. The projected transverse momentum distribution of the "wrong" sign muon is considerably higher than that of the typical hadron. The transverse momentum is defined as being out of the plane defined by the neutrino and the right sign muon. Furthermore the distribution appears to cut off around 1 GeV/c. The definition of the transverse momentum and its actual distribution (on a semi-log scale) are illustrated in Fig. 11.

Soon after the initial observation of the $\mu^+ \mu^-$ events by the HPWF group, these results were corroborated by an independent experiment of

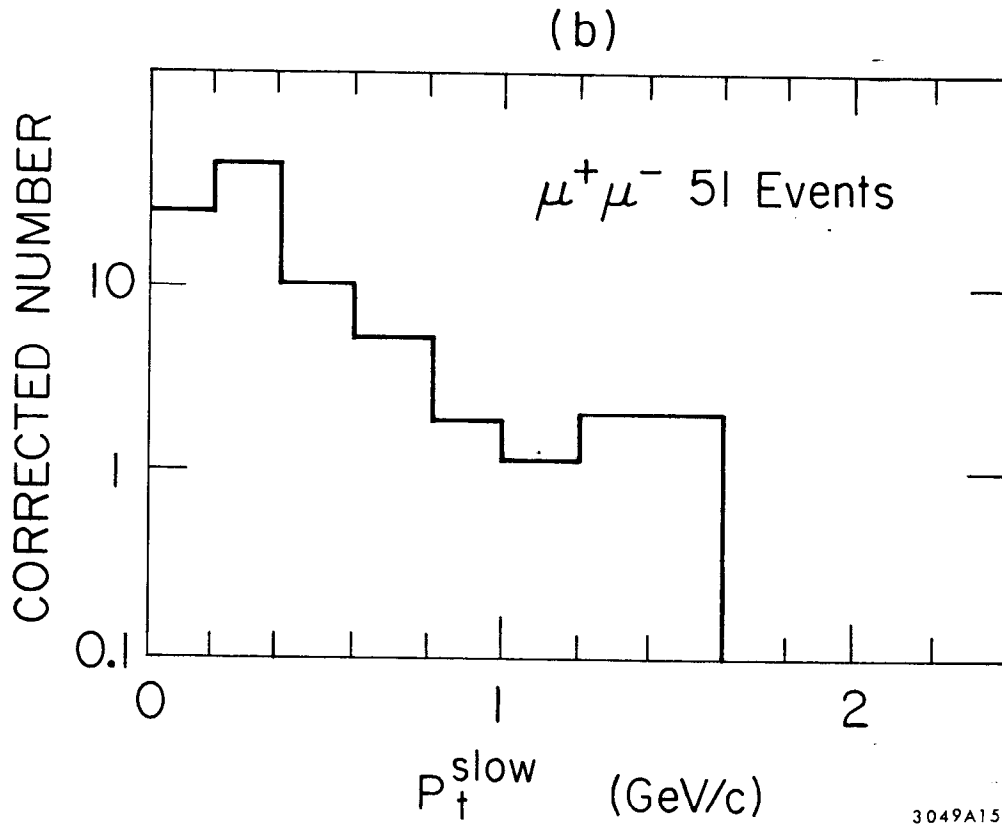
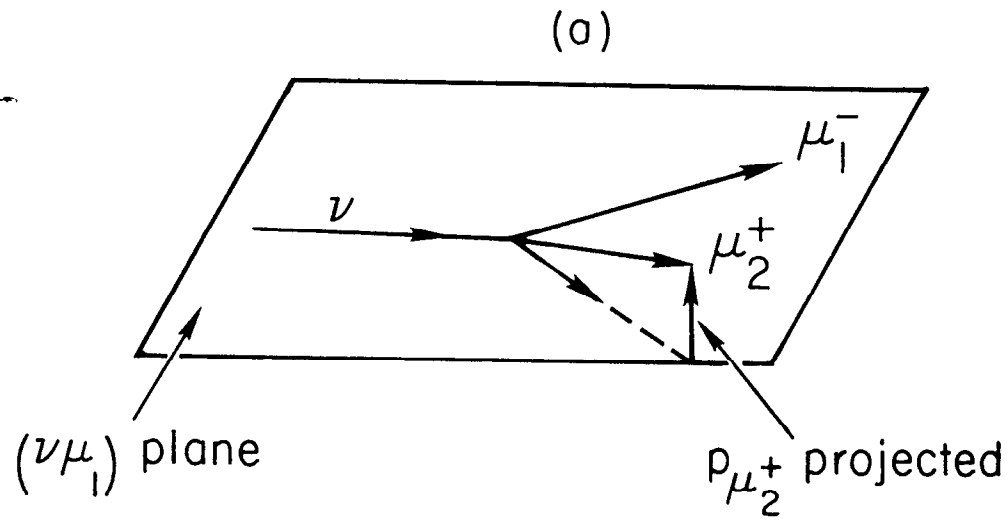


Fig. 11 a) Definition of the transverse momentum variable.
b) Distribution of the events in the transverse momentum variable.

the Cal Tech-Fermilab group.²⁶⁾ Here the muon identification was obtained by the requirement of penetration through 2m of Fe, or effective cut on the muon momentum of 3 GeV. The fundamental limitation of this experiment was the small solid angle subtended by the 5' diameter magnet at the end of the apparatus. Thus in a large number of dimuon events either one or both of the muons could not have their charge identified. The overall experimental situation is summarized in Table V.

TABLE V

Number of single and double muon events.

Beam	1 μ	2 μ	"Right Sign" Identified	Both Charges Identified
ν	2313	19	8	4
$\bar{\nu}$	446	2	2	0

One can again draw several conclusions from the data, supporting those of the HPWF group.

1. There seems to be an excess of observed 2 μ events beyond the number expected from π or K decay as illustrated in Fig. 12.
2. All of the events where both momenta are measured satisfy

$$P_{\mu^-} > P_{\mu^+} \text{ and give}$$

$$\frac{\langle P_{\mu^-} \rangle}{\langle P_{\mu^+} \rangle} = 3.6$$

3. As seen from Fig. 13, the ratio of 2 μ to single μ events appears to increase with energy; more specifically it appears to be considerably higher for the ν 's originating from K decay ($\bar{E}_{\mu} \approx 150$ GeV) than for those from the π decay ($\bar{E}_{\nu} \approx 50$ GeV). Again one must ask how much of this effect is due to experimental bias as opposed to any threshold phenomena. The answer to that question must await better data but several remarks can be appropriately made here. The $P_{\mu} > 3$ GeV cut is already a severe detection limitation at low energy but one should emphasize that for most

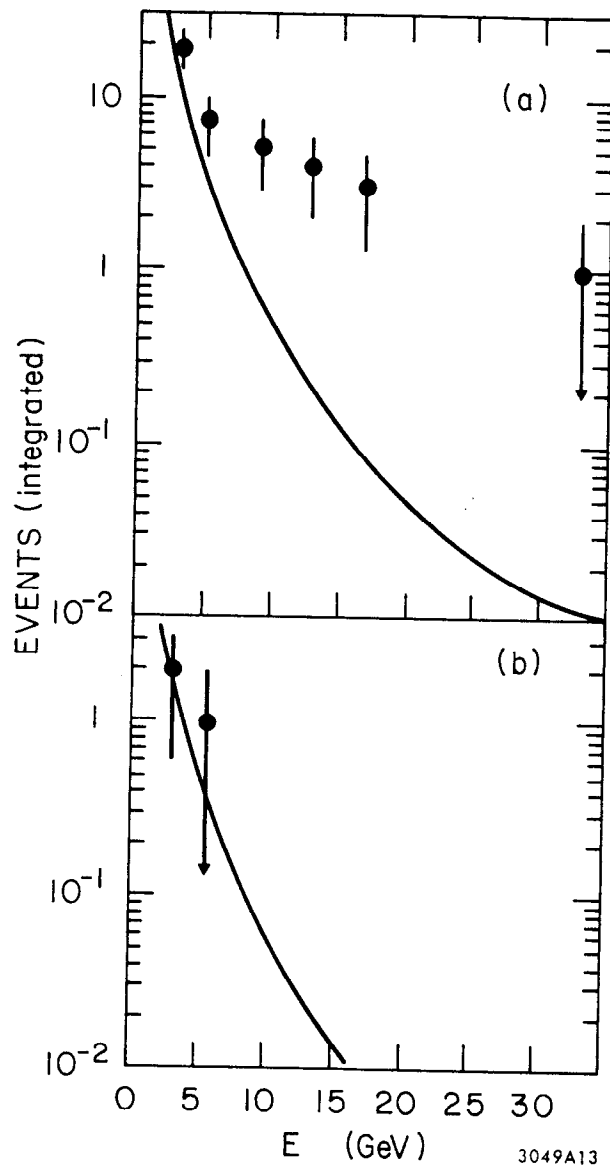


Fig. 12 Number of dimuon events with $E_{\mu^+} > E$ from neutrino (a) and anti-neutrino (b) running. The curves represents the Monte Carlo calculation of the number of μ 's arising from π or K decay.

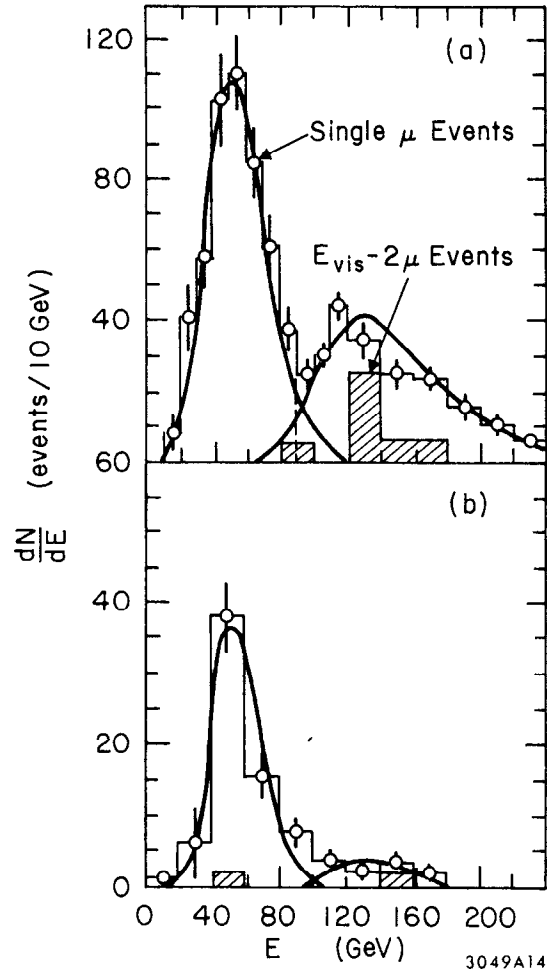


Fig. 13 Total energy distribution of single μ and 2μ events having the "right sign" muon through the spectrometer for the ν (a) and $\bar{\nu}$ (b) runs.

configurations the effective cut is even higher. This is due to the fact that for typical P_T 's of the second muon ($\langle P_T^+ \rangle = 1.2$ GeV/c for the 4 events with both μ 's through the magnet) the probability at low incident energies that the muon will leak out through the side of the apparatus before it has a chance to penetrate 2 m of iron is quite high. This will increase the P_{μ} cutoff to somewhere around 6 GeV/c for the CITF geometry, strongly suppressing the probability of observing and identifying dimuon events at the lower energies.

We end the discussion of the $\mu^+\mu^-$ data by summarizing the results from Serpukhov.²⁷⁾ The groups there performed 3 runs: 2 with different ν spectra and one with a $\bar{\nu}$ beam. The spectra for these three runs are illustrated in Fig. 14. As can be seen ν run 2 has the high energy end of ν spectrum enhanced compared to run 1. By defining a muon as a particle penetrating 0.48 m of Fe one can obtain a preliminary ratio of $2\mu/\mu$ events for the three runs. These results are indicated in Table VI and show a significant rise of this ratio when the high energy part of the spectrum is enhanced.

TABLE VI

Number of single and double muon events in Serpukhov experiment.

Run	Beam	No. of Protons	# 1μ	# 2μ	$R = \frac{2\mu}{\mu}$
1	ν	9.4×10^{16}	11830	91	$.77 \times 10^{-2}$
2	ν	13.6×10^{16}	8270	173	2.09×10^{-2}
3	$\bar{\nu}$	15.5×10^{16}	3600	19	$.53 \times 10^{-2}$

The majority of the " 2μ " events, however, correspond to the events where the other muon is either a π or K decay product or a hadron punch-through. Accordingly, for each run a Monte Carlo calculation was performed to calculate the expected number of " 2μ " events due to such

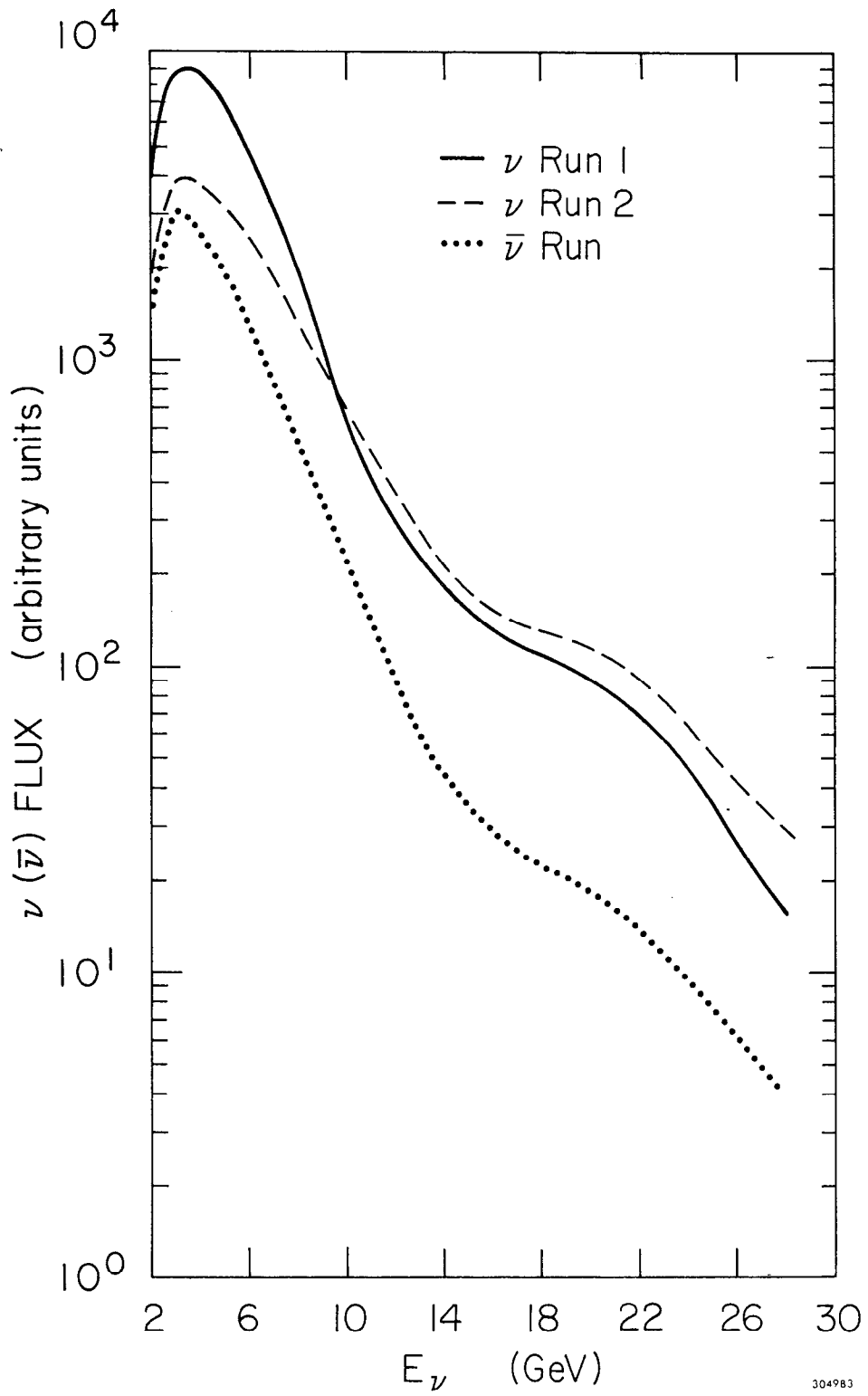


Fig. 14 The ν and $\bar{\nu}$ spectra for the three Serpukhov runs.

conventional mechanisms as a function of the definition of the muon. The variable parameter in defining the muon was the amount of Fe that was required for the muon to penetrate. The results of this calculation, as well as the experimental data, are displayed in Fig. 15. A significant deviation is seen for run 2 for the muons above a certain energy, which the authors interpret as the evidence for dimuon production by neutrinos involving a new mechanism.

It is difficult to quote an absolute rate but the authors claim that their results are consistent with

$$\frac{\mu^+ \mu^-}{\mu} \approx 10^{-2}$$

for neutrino energies above 10 GeV.

c. Interpretation of the Dilepton Data. Before discussing the comparison of the dilepton data with the charm picture one should briefly dispose of some of the other possible mechanisms that could have generated dilepton events (see Fig. 16).

1. neutral current $+ V^0 \rightarrow \mu^+ \mu^-$. This process would give dimuons with unique (or a set of unique) mass values and could not (in the context of conventional ideas) give μe events. The observed continuum of the $M_{\mu\mu}$ spectrum and the presence of μe events excludes this hypothesis.
2. $\nu\mu \rightarrow \nu\mu$ scattering. This process is very interesting in its own right and as such has been calculated extensively.²⁸⁾ The observed rate is far too large to account for the observed events and some of the theoretical distributions differ greatly from the observed ones. Specifically, these 4-fermion interaction events should be quasielastic, i.e. display a low total hadronic energy and give $M_{\mu\mu}$ mass peaked near 2μ masses. Both of the experimental distributions deviate markedly from these predictions.

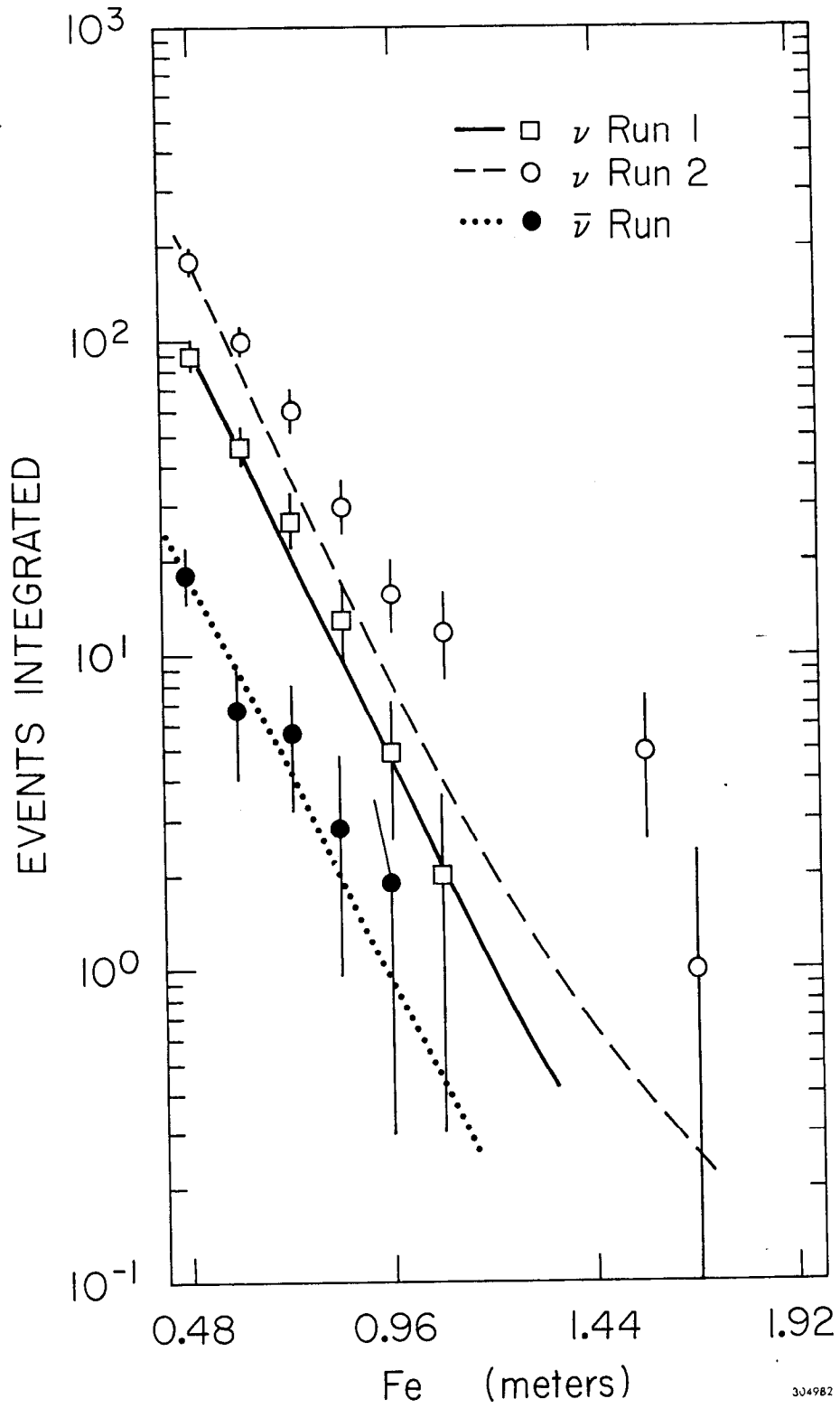
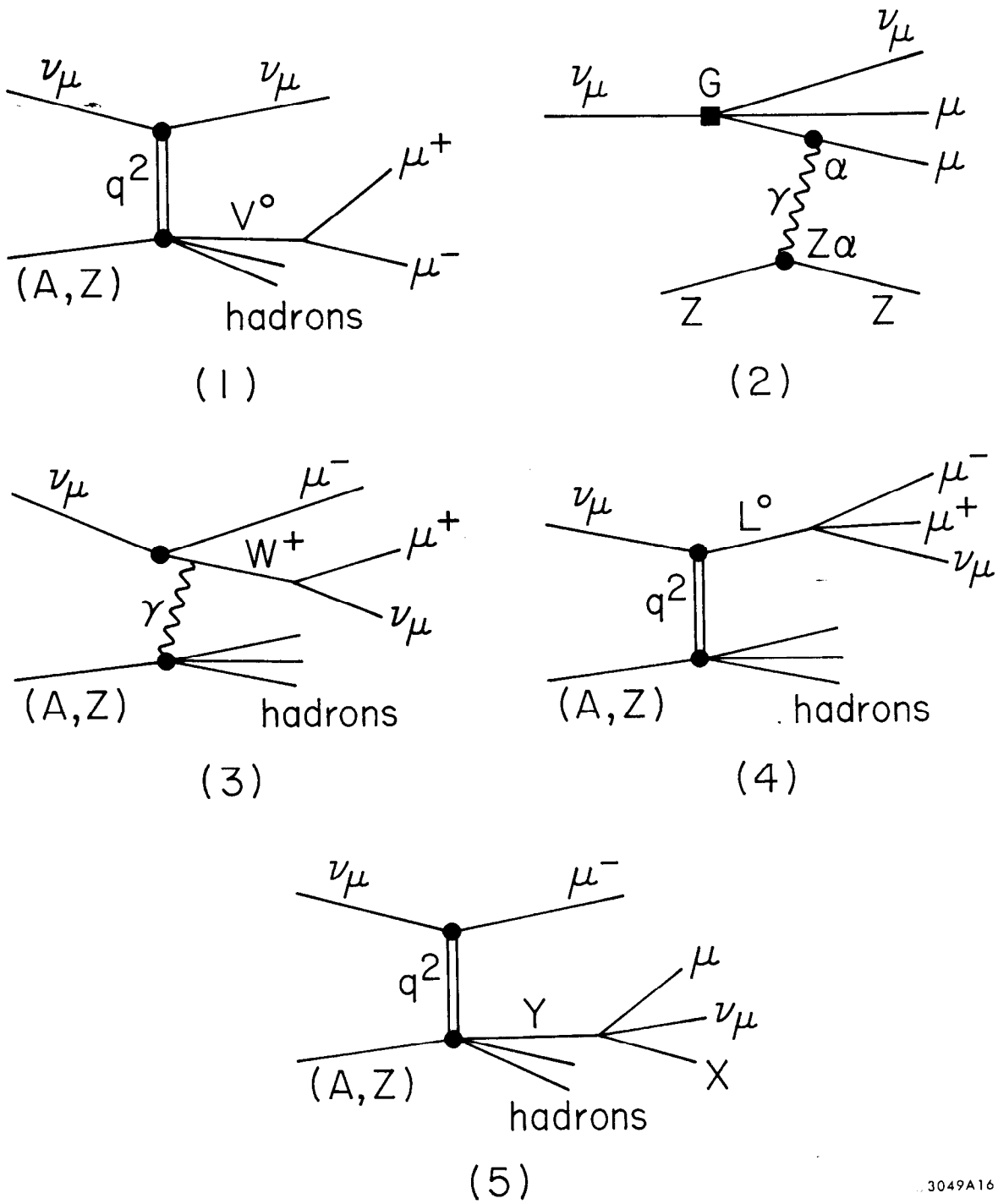


Fig. 15 Comparison of the observed number of "dimuon" events with the number calculated from π and K decay and hadron punchthrough.

304982



3049A16

Fig. 16 The possible mechanisms for the dimuon production.

3. W boson production. If the W boson is responsible for the observed dilepton events, then its mass would be in the vicinity of 5 GeV. This would have two important repercussions, both of which are in disagreement with the data. The transverse momentum of μ^+ would be about a factor of 2 wider than the observed one and one would see important propagator effects in the total cross section, none of which are seen. In addition one would expect $P_{\mu^+} > P_{\mu^-}$ contrary to the experiment.
4. neutral heavy lepton production. This has been an interesting theoretical possibility and has been studied rather extensively. There are now, however, several strong arguments against this possibility. Firstly, in heavy lepton decay both muons would be produced locally and thus $M_{\mu\mu}$ spectrum should be independent of the energy of the incident neutrino. The opposite appears to be true, the mass spectrum becoming wider with increasing neutrino energy.

Even more important is the argument put forth by Pais and Treiman²⁹⁾ which shows that on very general grounds the ratio

R defined by

$$R = \frac{\langle P_{\mu^-} \rangle}{\langle P_{\mu^+} \rangle}$$

must satisfy the condition $\frac{1}{2} < R < 2$ if we limit ourselves to

V, A couplings. In full generality the condition becomes

$$(9-4\sqrt{2})/7 \leq R \leq (9+4\sqrt{2})/7.$$

As discussed above, this prediction is in strong disagreement with the data and thus appears to exclude the heavy lepton hypothesis. The experimentally observed ratio R may conceivably need some correction due to contamination by μ 's from π or K decays and possible confusion as to the ν or $\bar{\nu}$ source of the event but it is highly unlikely that these numbers could be brought anywhere close to the Pais Treiman limit.

5. new hadron production. This then brings us to the most likely interpretation of these events namely a production of a hadron with new quantum numbers, which subsequently decays leptonically (or semileptonically). It remains to ask the question whether the data are self consistent and whether they agree with the several predictions of the charm (GIM) model.³⁰⁾

Association with strange particles - One might expect that at low energies, i.e. in Gargamelle exposure, the charmed particles would be produced off valence quarks, and thus unaccompanied by strange particles. At these low energies we would expect prevalence of charmed baryons and only one strange particle in the final state. At higher energies e.g. 15' exposure at Fermilab, production off sea quarks might become more important resulting in 2 strange particles in the final state. Certainly, the correlation with strange particles appears to be well established experimentally in both experiments; there may be even indications of too high a kaon yield at higher energies if one assumes that $\bar{N}_{K^0} = \bar{N}_{K^+}$. However, the statistics are too limited on this point to say that the GIM model is violated here.

Spectra - We can compare here with a specific model of Barger and Phillips that assumes a charmed meson mass of 2.3 GeV and a decay into a Kev final state without any hadronic form factor. The agreement of the HPWF data with these predictions is quite good, as can be seen from Fig. 17.

Rate - What we observe is a product of charmed particle production rate times its semileptonic branching ratio, i.e.

$$\frac{\sigma_{\text{charm}}}{\sigma_{\text{Ch Curr}}} \cdot \frac{B_{\text{charm}} \rightarrow \ell \nu \text{ hadrons}}{B_{\text{charm}} \rightarrow \text{all}}$$

where the branching ratio is an average over the several possible

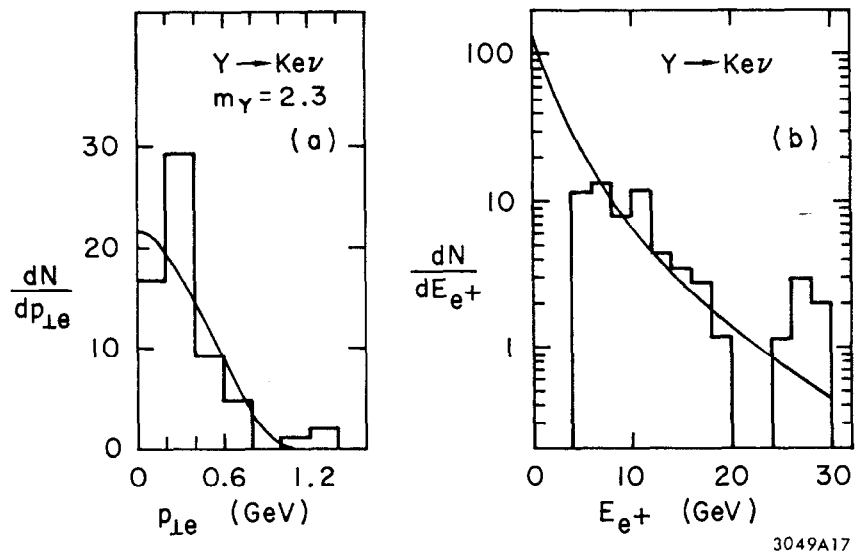


Fig. 17 Comparison of the predicted transverse momentum distribution (a) and the laboratory momentum distribution (b) of the electron from D decay with the observed μ^+ distributions from the HPWF experiment.

charmed particle ground states weighed by their production cross section. According to the basic ideas discussed above we would expect:

$$\frac{\sigma_{\text{charm}}}{\sigma_{\text{c.c.}}} \approx 10\%$$

Furthermore, a reasonable guess³¹⁾ for the leptonic branching ratio is also about 10%, giving a product of 1%. In comparing with the data one must keep in mind that the dimuon data needs an appreciable correction because of the muon energy cutoff. In the Barger-Phillips model, that correction factor is about 3. Thus we conclude that there exists a fair agreement, with a discrepancy of maybe a factor of 2 or 3 between μe and $\mu\mu$ data, the $\mu\mu$ data being slightly high.

Threshold - for the process

$$\nu_{\mu} N \rightarrow C \mu^{-}$$

the threshold is $P_{\nu} = 2.5 \text{ GeV}/c$ if one takes $M_c = 2.25 \text{ GeV}$. The fact that all three GGM events occur above 3 GeV is consistent with this picture.

M_{Ke} and $M_{\Lambda e}$ spectra - if both the electron and the strange particle originate from the decay of one particle then the effective mass of this di-particle system must be less than the mass of the parent. The fact that the mass of this system is below 2 GeV for all the measurable observed events indicates that here too the agreement with the GIM model is quite good.

d) Dileptons of Same Sign. The HPWF group have also reported observation of 7 $\mu^{-}\mu^{-}$ and 3 $\mu^{+}\mu^{+}$ events. The natural question here is again whether these events represent a new phenomenon or come from an uninteresting source like a secondary π or K decay. The fact that 7 out of 10 events (see Table VII below) came from the iron hadron filter and only 3 are produced in much lighter liquid scintillator appears to argue against

TABLE VII

Parameters of the $\mu^-\mu^-$ and $\mu^+\mu^+$ Events

Target	E_H (GeV)	P_1 (GeV/c)	P_2 (GeV/c)	θ_{12} (mr)	P_{t1} (GeV/c)	P_{t2} (GeV/c)
Filter		53.3	11.5	111	.58	.16
Filter		30.6	14.0	67	.6	.6
Filter		57.9	38.8	89	.34	.14
Filter		25.2	12.8	81	.09	.36
Calorimeter	123	51.7	6.1	65	1.9	.38
Filter		14.1	5.5	300	4.0	1.1
Calorimeter	22	19.9	4.2	295	2.7	.33
Calorimeter**	22	8.8	4.8	68	.36	.13
Filter**		17.5	9.1	255	.17	.37
Filter**		28.5	2.4	125	.05	.33

** $\mu^+\mu^-$

the decay hypothesis. On the other hand both the momentum distribution and the P_T distribution of the lower energy muon appear lower than in the case of $\mu^+\mu^-$ events, indicating that the π -K decay may not be an insignificant source. Finally one must remember that the HPWF Monte Carlo analysis of the $\mu^+\mu^-$ events indicated that within one standard deviation about 25% of them could be due to π or K decay, a fraction that corresponds to a total number that is higher than the observed number of $\mu^{\pm\pm}$ events.

Nevertheless, it is interesting to speculate about the possible origin of these events if they do not come from π or K decay. An obvious possibility would be the associated production of the same new particles that are responsible for $\mu^+\mu^-$ events. This would be very exciting, as it would point to a relatively high cross section for new particle production in hadronic interactions. Of course, only time and better statistics will resolve this question.

VI. $\Delta S/\Delta Q$ and STRANGE PARTICLE PRODUCTION

As mentioned previously, charm production should exhibit itself as an increase in strange particle production, due both to the high probability of producing strange particles in association with charm, as well as due to the supposed preference of charm decay into strange particles.

The Table VIII below gives the fractions of all charged current events which have at least one strange particle associated with them, for different average energies of the neutrino beam. As can be seen there does

TABLE VIII

Fraction of charged current events with 1 or more strange particles.

Chamber	Fill	Beam	$\overline{E}_{\nu, \bar{\nu}}$	Fraction	Reference
12'	H,D	ν	2 GeV	$7 \pm 4\%$	32
GGM	Freon	ν	> 1 GeV	$8 \pm 2\%$	33
7'	H,D	ν	> 4 GeV	$8 \pm 3\%$	8
15'	H	$\bar{\nu}$	23 GeV	$18 \pm 7\%$	20
25'	H	ν	38 GeV	$16 \pm 3\%$	34

indeed appear to be a rise with the energy. The question remains, however to what extent that effect can be ascribed to purely kinematical effects like the simple increase in multiplicity in energy. The measurement charged prong multiplicity³⁵⁾ increases from an average value of 3.84 for $15 < E_{\nu} < 30$ GeV to 5.25 for $E_{\nu} > 50$ GeV. This increase thus appears to be too slow to account for the whole effect and the rise in the strange particle yield probably does have a dynamical explanation.

We turn next to the question of $\Delta Q/\Delta S$ violation as evidence for charmed particle production. The evidence against $\Delta Q = -\Delta S$ comes from the absence of several decay modes, namely

- a) in K^0, \bar{K}^0 system $\bar{K}^0 \not\rightarrow e^+$ and $K^0 \not\rightarrow e^-$
- b) absence of $\Sigma^+ \rightarrow n \ell^+ \nu$ mode
- c) absence of $K^+ \rightarrow \pi^+ \pi^+ e \nu$ mode.

The data is good enough to exclude the $\Delta Q/\Delta S$ amplitude at the level of 1% or so in amplitude. Thus evidence for its violation in ν interactions would be a strong evidence for charm production. This rule would appear to be violated if the charmed particle production proceeded off a valence quark, resulting in $\Delta S=0$ and $\Delta Q=\Delta C=1$ in the production process. If subsequently the charm particle decayed via strange particle mode, the decay would obey $\Delta C=\Delta S=-1$, resulting in the overall $\Delta Q=-\Delta S$. This process might be expected to dominate close to threshold since the charm production off the quark-antiquark sea is expected to become more important at higher energies.

The now famous BNL event, illustrated in Fig. 18, is very likely one of the first examples of production and decay of a charmed particle.³⁶⁾ The observed event fits the interpretation

$$\nu p \rightarrow \mu^- \Lambda \pi^+ \pi^+ \pi^+ \pi^-$$

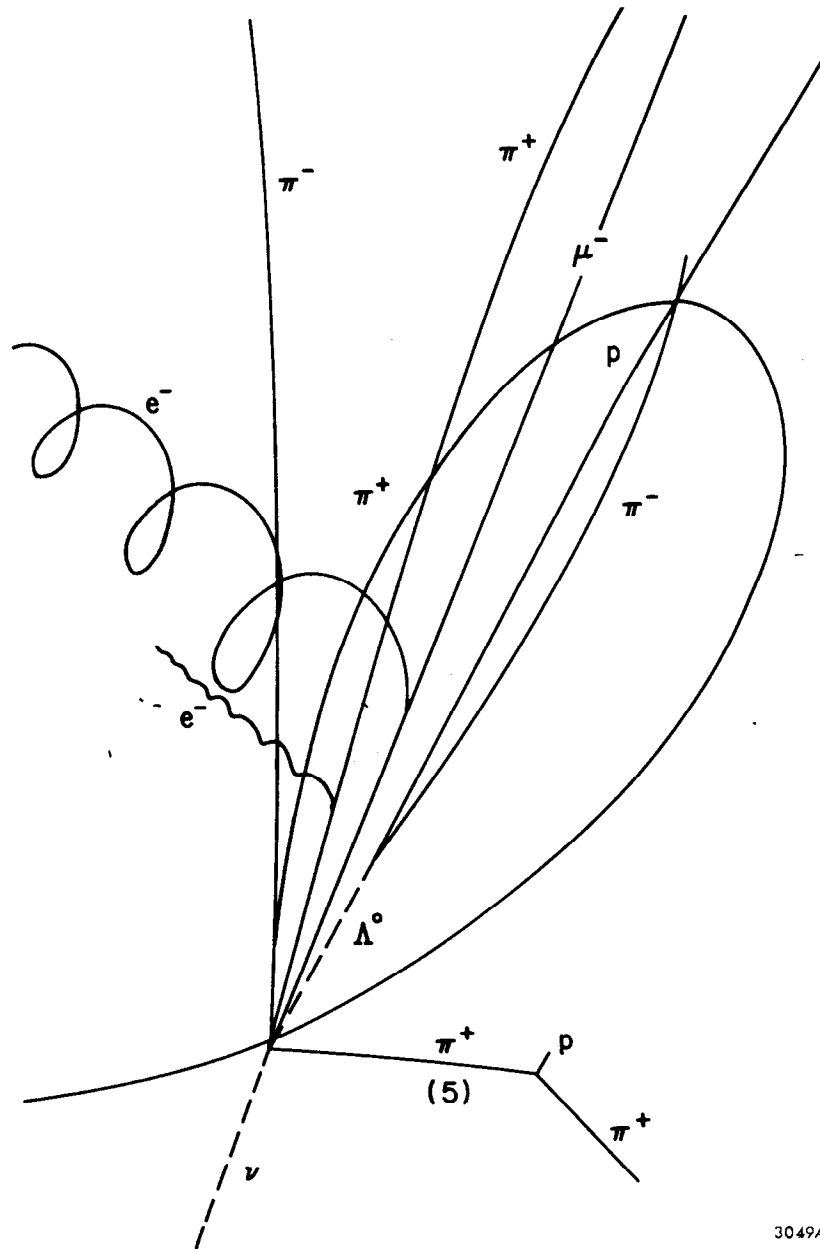
and is reported to have only a 3×10^{-5} probability for other interpretations. The total sample of charged current events out of which this event was found included 335 events, 14% of which had $E_\nu > 4$ GeV, and 1.5% $E_\nu > 20$ GeV.

If one interprets the event as

$$\nu p \rightarrow \mu^- \begin{array}{l} C^{++} \\ \downarrow \\ \Lambda \pi^+ \pi^+ \pi^+ \pi^- \end{array}$$

then the mass of the charmed baryon C turns out to be 2426 ± 12 MeV.

Corroborative evidence for this process was looked for²⁰⁾ at Fermilab in the 15' bubble chamber filled with liquid hydrogen. Because of higher energy the probability of missing π^0 's is very high and thus one can only make the argument on a statistical basis. In the total exposure 17 single Λ events were found and 3 events with both a Λ and a K_S^0 . If one assumes K_S^0, K^+ production equality then the calculated number of $\Delta Q=-\Delta S$ events turns out to be $17-5.3 \times 3=0.8$. Thus at a 90% confidence level one can put



3049A1

Fig. 18 The BNL event appearing to violate $\Delta Q = \Delta S$ rule.

the limit on the $\Delta Q = -\Delta S$ process at less than 3.6% of all charged current events for neutrino energies above 10 GeV.

The search for $\Delta Q = -\Delta S$ is equally difficult in Gargamelle exposure because of the much worse measuring accuracy and a complicated target, which make kinematical fitting impossible. In that exposure out of 1450 charged current events with hadronic mass W satisfying $W > M_K + M_\Lambda$, 28 single Λ events were found with a detection probability of $52 \pm 4\%$. All of them, however, are consistent with having another strange particle.³³⁾

VII. SCALING VARIABLE DISTRIBUTIONS

We start our discussion here with a very brief review of the standard formulas used in discussing neutrino interactions. The scaling variables x and y are defined by

$$x = -q^2/2\nu \text{ and } y = \nu/m_p E_\nu$$

where ν is the measure of inelasticity defined by $\nu = m_p(E_\nu - E_\mu)$.

The 2 dimensional scattering formula then becomes

$$\begin{aligned} \frac{d^2 \sigma_{\nu, \bar{\nu}}}{dx dy} &= \frac{G^2 m_p E_\nu}{\pi} \left[F_2(x)(1-y) + 2x F_1(x) \frac{y^2}{2} \mp x F_3 y \left(1 - \frac{y}{2}\right) \right] \\ &= \frac{G^2 m_p E_\nu}{\pi} F_2(x) \left[\left(1-y + \frac{y^2}{2} (R+L) \mp y \left(1 - \frac{y}{2}\right) (L-R) \right) \right] \end{aligned}$$

$$\text{with } R = \sigma_R/(\sigma_R + \sigma_L + 2\sigma_S) \text{ and } L = \sigma_L/(\sigma_R + \sigma_L + 2\sigma_S)$$

and the $-$ sign in the original expression corresponding to the ν scattering and the $+$ sign to antineutrino scattering. The σ_R , σ_L , σ_S are the cross sections for the right handed, left handed, and scalar scattering. The F 's are scaling functions related to the quark antiquark distributions in the nucleon. The F_1 and F_2 can be obtained from the deep inelastic electron scattering, but F_3 , representing V,A interference must be obtained from the difference between neutrino and antineutrino scattering.

It is conventional to define quark, antiquark distributions $q(x)$, $\bar{q}(x)$ by

$$q(x), \bar{q}(x) = \frac{1}{2} F_2(x) \mp x F_3(x)$$

and a function $B(x)$ that is related to quark, antiquark asymmetry in the nucleon

$$B(x) = \frac{q(x) - \bar{q}(x)}{q(x) + \bar{q}(x)} = - \frac{x F_3(x)}{F_2(x)}$$

Finally, if the nucleon constituents (quarks) have spin 1/2, we have the Callan Gross relation $F_2(x) = 2 x F_1(x)$.

In terms of this nomenclature we can rewrite the equation for the differential distribution as

$$\frac{d^2 \sigma^{\nu}}{dx dy} = \frac{G_m^2 E_\nu}{\pi} \left[q(x) + \bar{q}(x)(1-y)^2 \right]$$

and a similar relation for $\sigma^{\bar{\nu}}$, with $q(x)$ and $\bar{q}(x)$ interchanged.

Alternatively we can write

$$\frac{d^2 \sigma^{\nu, \bar{\nu}}}{dx dy} = \frac{G_m^2 E_\nu}{\pi} \int F_2(x) dx \left[\left(1-y + \frac{y^2}{2}\right) \pm B y \left(1 - \frac{y}{2}\right) \right]$$

Now, in the quark model we can turn proton into a neutron by merely interchanging the down and up quarks. Since the neutrinos can interact only with the down quarks and antineutrinos with the up quarks, this statement leads to the conclusion that $F_1^{\nu p} = F_1^{\bar{\nu} n}$. Finally, since an isoscalar target (a good approximation for most nuclei) is composed of an equal number of neutrons and protons, we must have $F_1^{\nu} = F_1^{\bar{\nu}}$, a statement known as charge asymmetry. This right away leads us to the prediction that

$$\left. \frac{d\sigma^{\nu}}{dy} \right|_{y=0} = \left. \frac{d\sigma^{\bar{\nu}}}{dy} \right|_{y=0}$$

provided only that charge asymmetry holds, i.e. $F_2^{\nu}(x) = F_2^{\bar{\nu}}(x)$.

We can also see easily from the above formulas two other predictions based only on the validity of scaling. Clearly the integral over the functions of x and y is independent of energy if scaling holds and thus

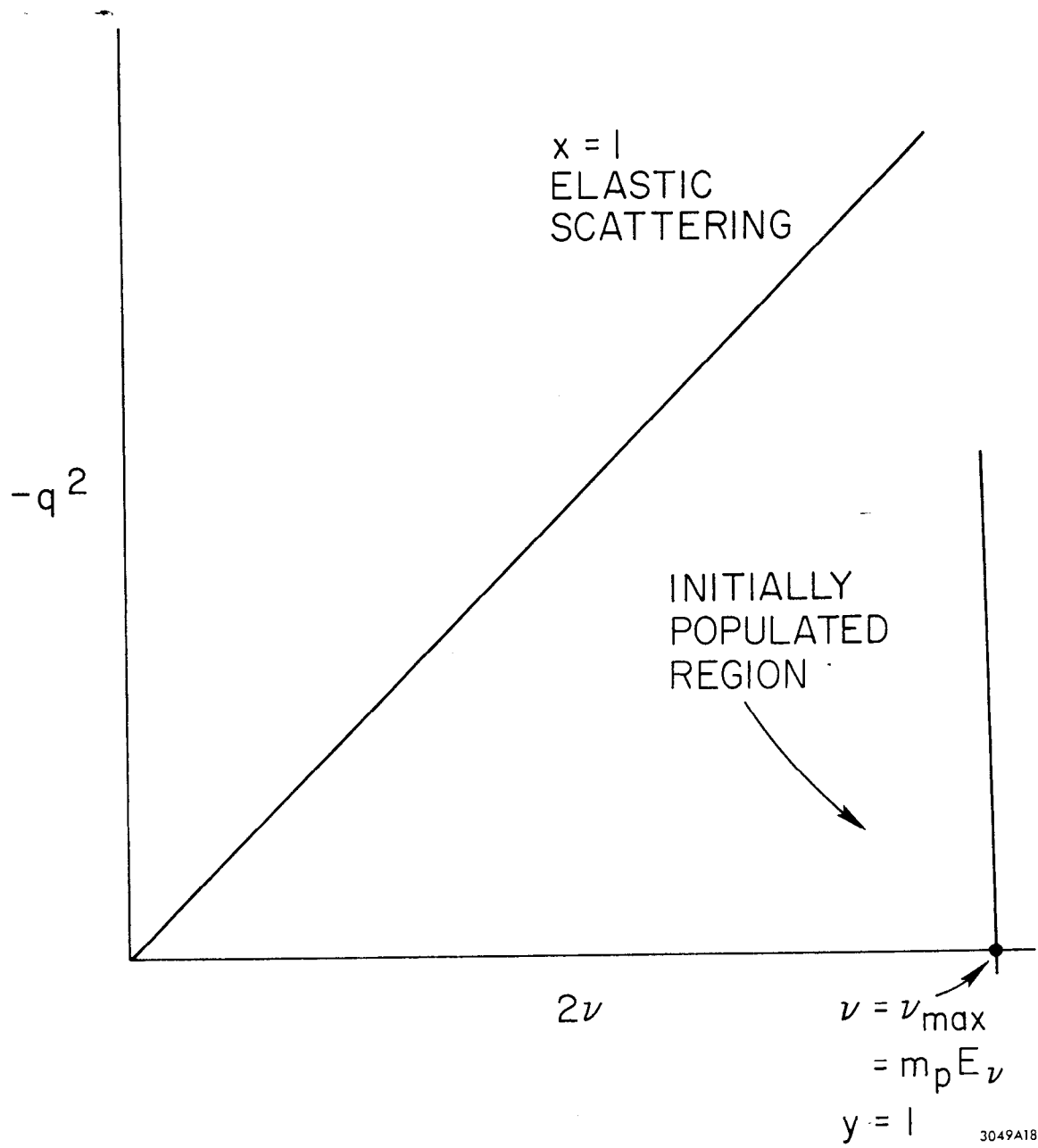


Fig. 19 q^2, ν plot for inelastic scattering.

Thus the events will first come in at the lower right hand corner, i.e. $x = 0, y = 1$. As we increase the energy, i.e. E_ν , the total hadronic energy E_H will also increase. Therefore, above threshold

$$1 \geq y \geq E_{th}/E_\nu$$

Consider now x behavior above threshold

$$\begin{aligned} x &= -q^2/2\nu \\ 2\nu x &= -q^2 = 2\nu - (W^2 - m_p^2) \\ &\leq 2\nu - 2m_p E_{th} \\ x &\leq 1 - \frac{m_p E_{th}}{\nu} \leq 1 - m_p \frac{E_{th}}{m_p y E_\nu} \leq 1 - \frac{E_{th}}{y E_\nu} \end{aligned}$$

And thus the values of x will be limited to

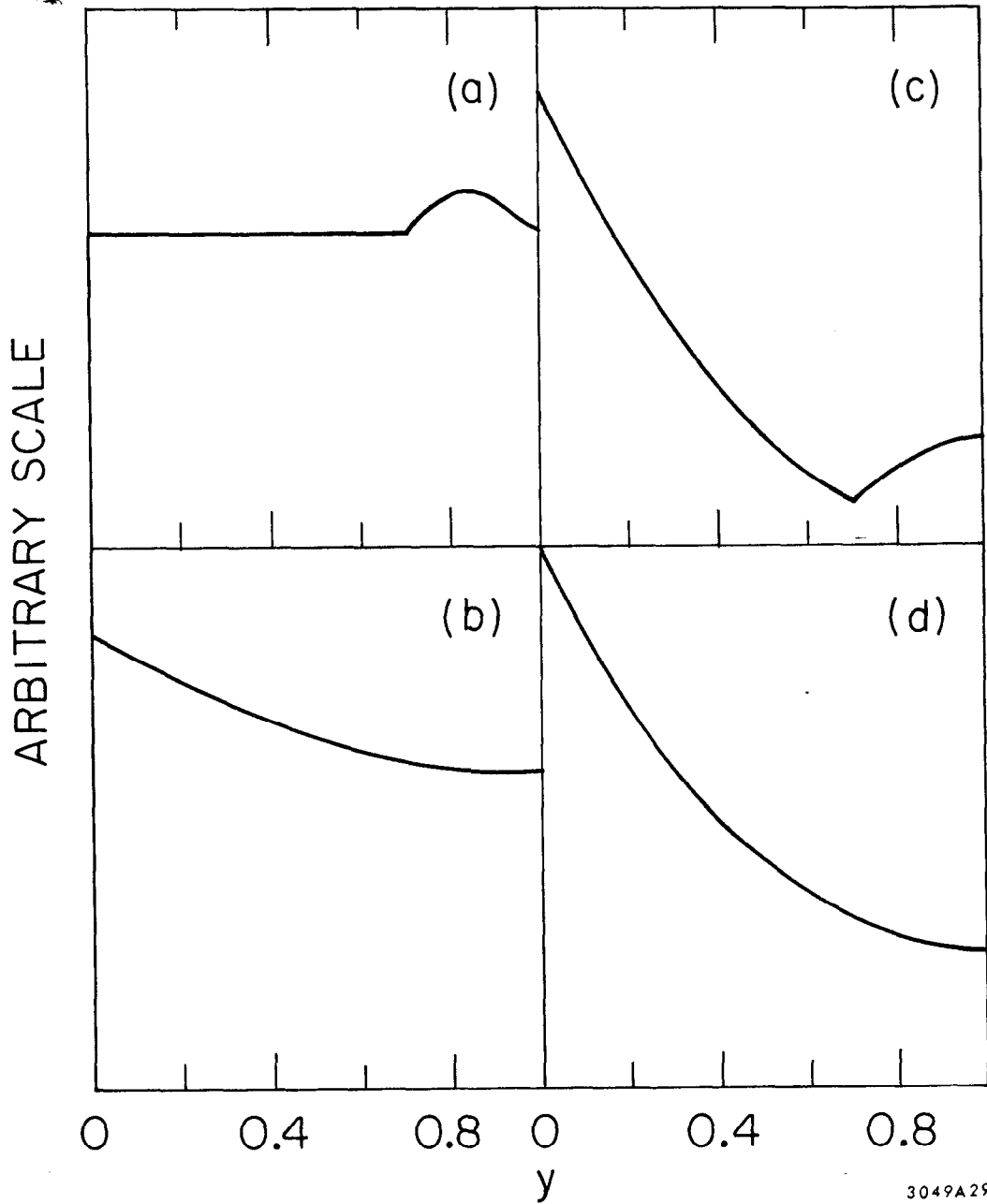
$$0 \leq x \leq 1 - E_{th}/yE_\nu$$

For completeness we derive also the expression for W , i.e. the total effective mass of the hadronic system.

$$\begin{aligned} y(1-x) &= \frac{E_H}{E_\nu} \frac{W^2 - m_p^2}{2\nu} \\ &= \frac{E_H}{E_\nu} \frac{W^2 - m_p^2}{2m_p E_H} = \frac{W^2 - m_p^2}{2m_p E_\nu} \\ W^2 &= m_p^2 + 2m_p y (1-x) E_\nu \end{aligned}$$

Thus the new particle production will tend to populate the kinematical region of high W , high y , and low x . Thus any new threshold phenomena can be seen much easier in the $\bar{\nu}$ interactions because the "old" physics suppresses the $y \approx 1$ region through the $(1-y)^2$ factor in the expression for the differential cross section.

We can illustrate in Fig. 20 the expected y behavior of both ν and $\bar{\nu}$ processes right above threshold for the new particle production and in the asymptotic region. It remains to ask about the expected magnitude of



3049A29

Fig. 20 Expected y distribution for ν (e,b) and $\bar{\nu}$ (c,d) right above threshold for new particle production (a,c) and in the asymptotic region (b,d). The curves are meant to be only qualitative.

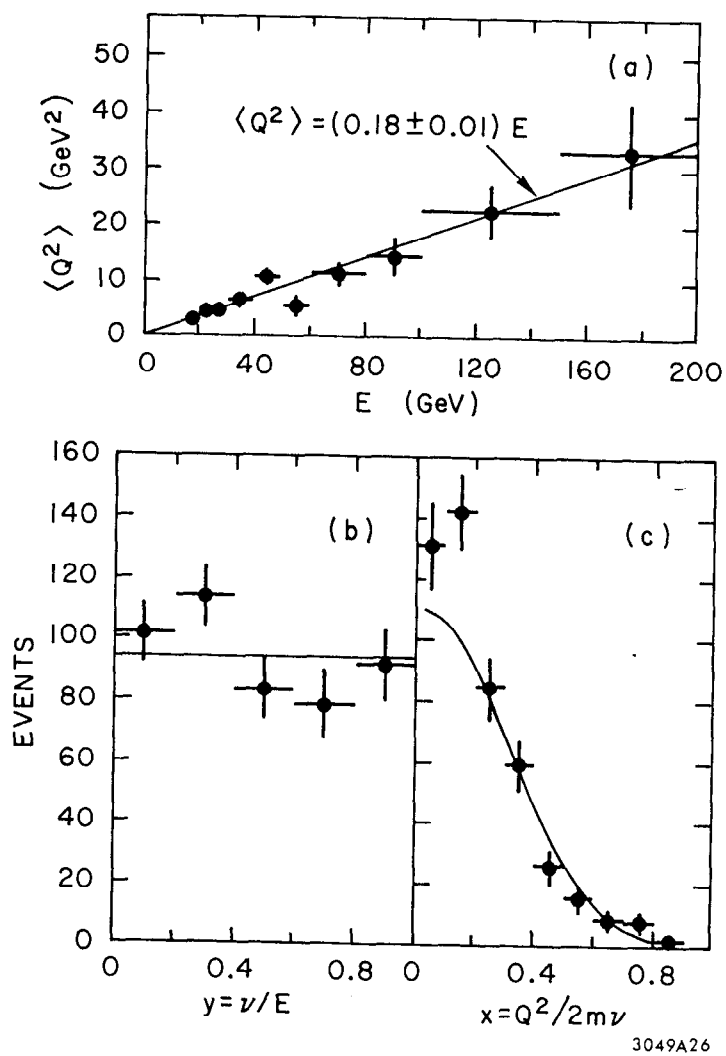
these effects. The answer here clearly depends on the specific model of the new particle production;³⁷⁾ the charm picture predicts that these effects cannot be large because:

1. $\sin^2 \theta_c$ is small (≈ 0.05) and thus production off valence quarks is suppressed.
2. the $q\bar{q}$ sea is small ($\approx 5-10\%$ according to the analysis of low energy interactions) and thus production from the s or \bar{s} quarks is also small. This statement assumes scaling, i.e. ability to extrapolate to high energies the low energy results on $q(x)$ and $\bar{q}(x)$ distributions.

We turn now to the discussion of the data, starting with a review of the bubble chamber experiments. Compared to the electronic experiments, these have in common relatively low statistics, and a lower average neutrino energy since all of the exposures have been done with the horn beam.

The Fermilab-Michigan group has analyzed³⁸⁾ some 450 charged current events representing neutrino interactions in the hydrogen filled 15' bubble chamber. The data, displayed in Fig. 21, is in good agreement with scaling predictions with some small excess of events near low x . A natural interpretation for this phenomenon, if high statistics will indeed uphold its validity, is the scaling violation already seen in inelastic lepton scattering, both in electron scattering data at SLAC and more recently in muon scattering at Fermilab. In brief, the violation exhibits itself as an increase in $F_2(x)$ at low x as we go to higher q^2 and can be understood theoretically in terms of gluon bremsstrahlung models.

There have been two exposures of the horn $\bar{\nu}$ beam in the 15' chamber, one in a pure hydrogen fill, the other in a light neon-hydrogen mixture. The Argonne-Carnegie Mellon³⁹⁾ collaboration has studied 106 events in hydrogen with a mean neutrino energy of 23 GeV (see Fig. 22). The y distribution is consistent with $(1-y)^2$ form predicted by the simple quark model and the x



3049A26

Fig. 21 Results of the Fermilab-Michigan neutrino experiment.
a) average value of q^2 plotted as a function of energy
b) y distribution for the events in the 15-200 GeV region
c) x distribution for the events in the 15-200 GeV region.

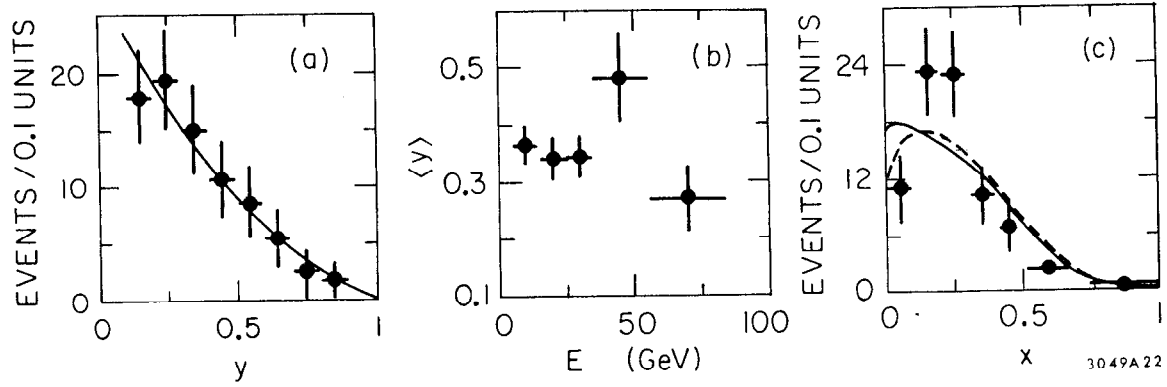


Fig. 22 Results of the Argonne-Carnegie Mellon $\bar{\nu}$ experiment a) y distribution, b) $\langle y \rangle$ as a function of E, and c) x distribution.

distribution agrees with the scaling function derived from lepton production data. It should be emphasized however that the data is heavily dominated by the low energy antineutrinos.

The Fermilab-ITEP-IHEP-Michigan groups have reported⁴⁰⁾ on 493 charged current antineutrino interaction with energies between 10 and 200 GeV in the light neon mixture. Their y distribution shown in Fig. 23 is consistent with the $(1-y)^2$ form plus a small constant term that is consistent with the amount of the antiquark component derived from the low energy data. The x distribution shown in Fig. 24 is consistent with the $F_2^{\text{ed}}(x)$ obtained at SLAC except for some enhancement at low x . The authors argue that this behavior would be expected in the region where the antiquark contribution is large (i.e. low x) because of a relatively higher cross section of the antineutrinos on antiquarks. Whereas the quark and antiquark components contribute equally to inelastic lepton scattering, the antiquarks are enhanced in antineutrino scattering by a factor of 3 resulting from the difference in y distributions.

The two electronic experiments providing information on the scaling variable distributions are those of the HPWF and CITF collaborations. The original indications for onset of new phenomena came from the HPWF group⁴¹⁾ who reported significant deviations from the $(1-y)^2$ distribution for the antineutrinos above 30 GeV with $x < 0.1$. These data are displayed in Fig. 25. In addition, if one normalizes the data by assuming equal cross sections at $y=0$ for $x < 0.1$, then the data for $x < 0.1$ gives a cross section higher by about a factor of 3 than the $\bar{\nu}$ cross section, implying a breakdown of charge symmetry.

The more recent data⁴²⁾ strengthens the evidence for deviation from $(1-y)^2$ for higher energy $\bar{\nu}$ data, but there no longer appears to be strong evidence for a qualitatively different behavior below and above $x=0.1$. The authors analyze all the data with $x < 0.6$ and fit the y distributions

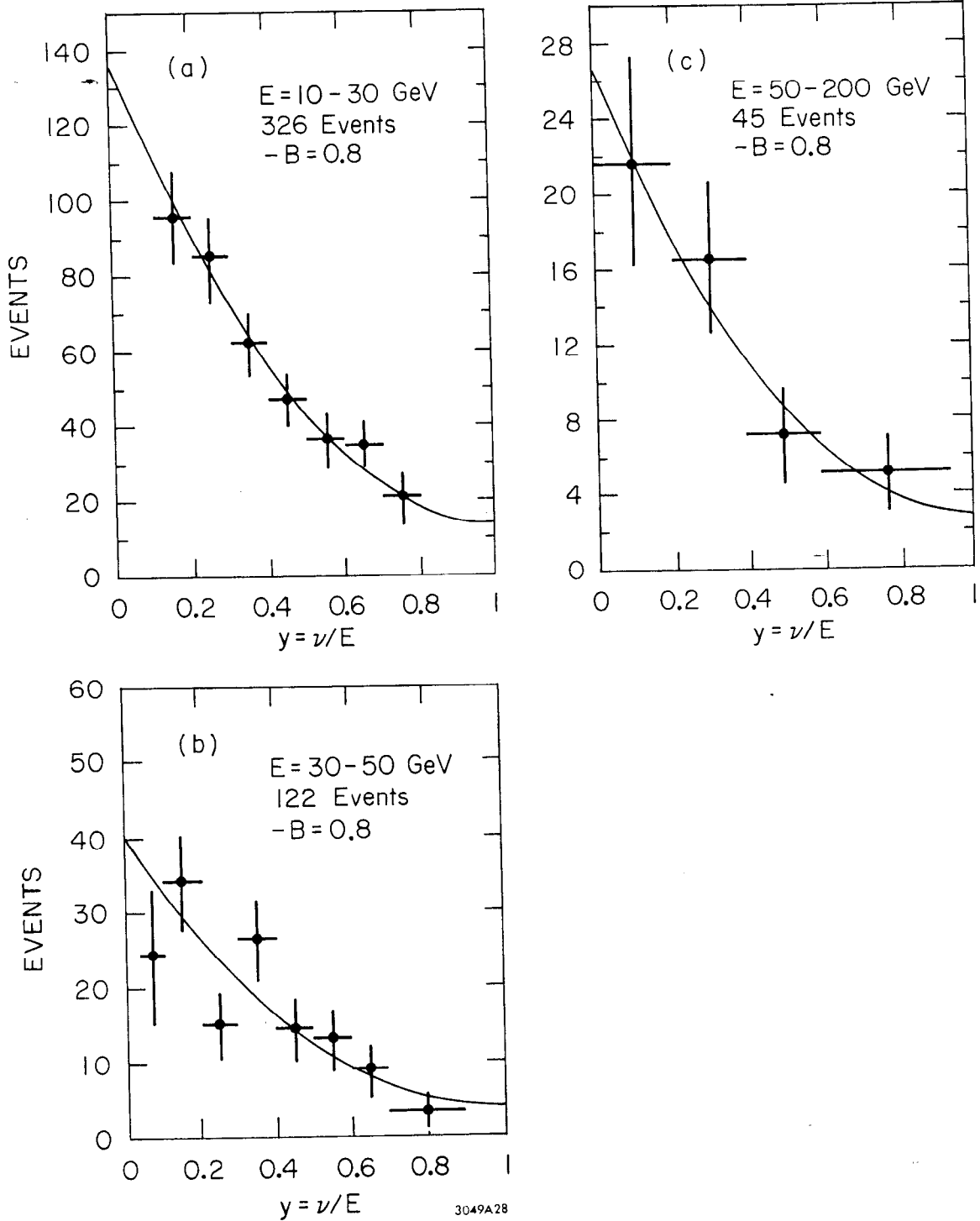


Fig. 23 y distribution for 3 different energy intervals for the Fermilab-IITP-IHEP-Michigan experiment.

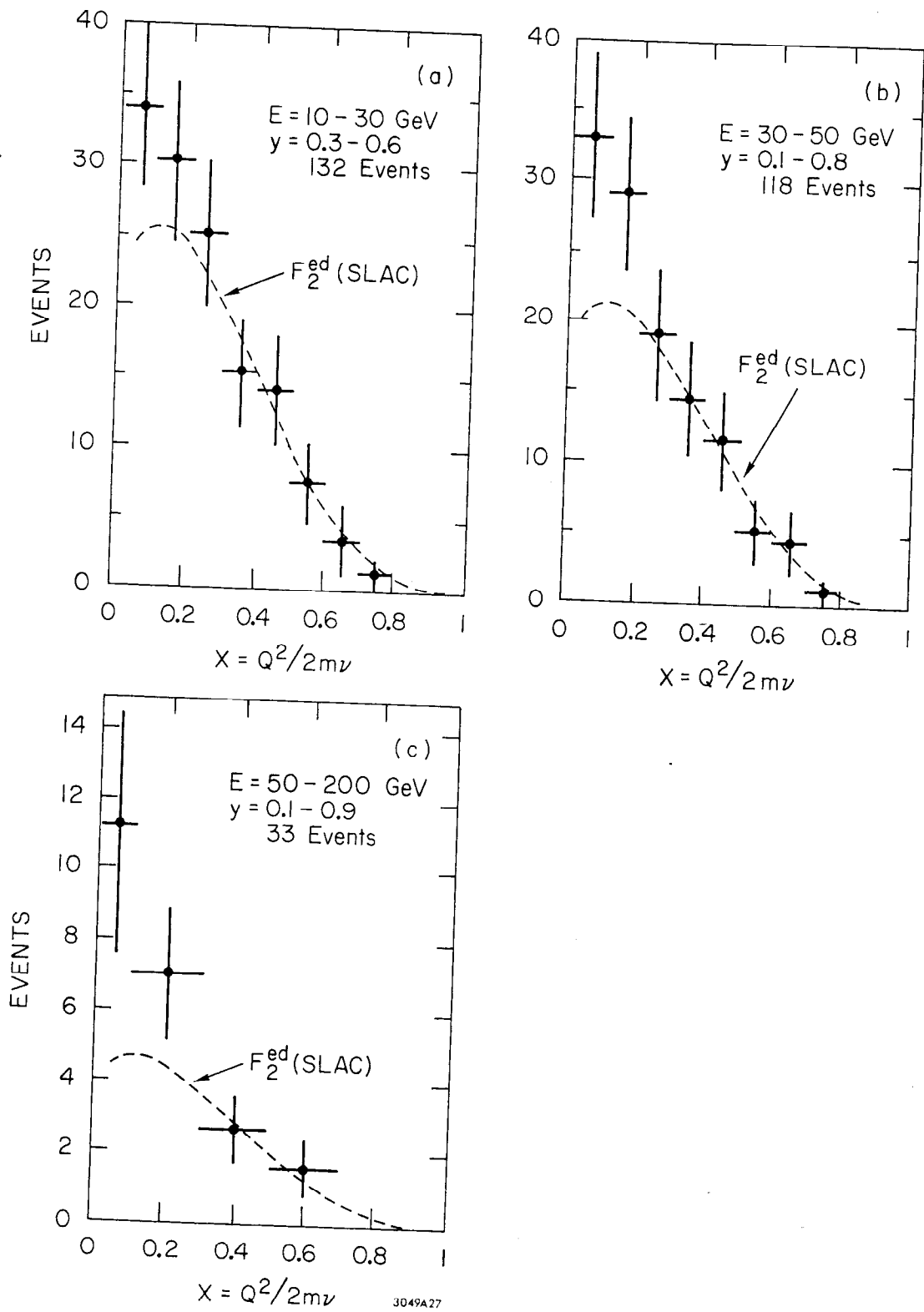


Fig. 24 x distribution for 3 different energy intervals for the Fermilab-IITP-IHEP-Michigan experiment.

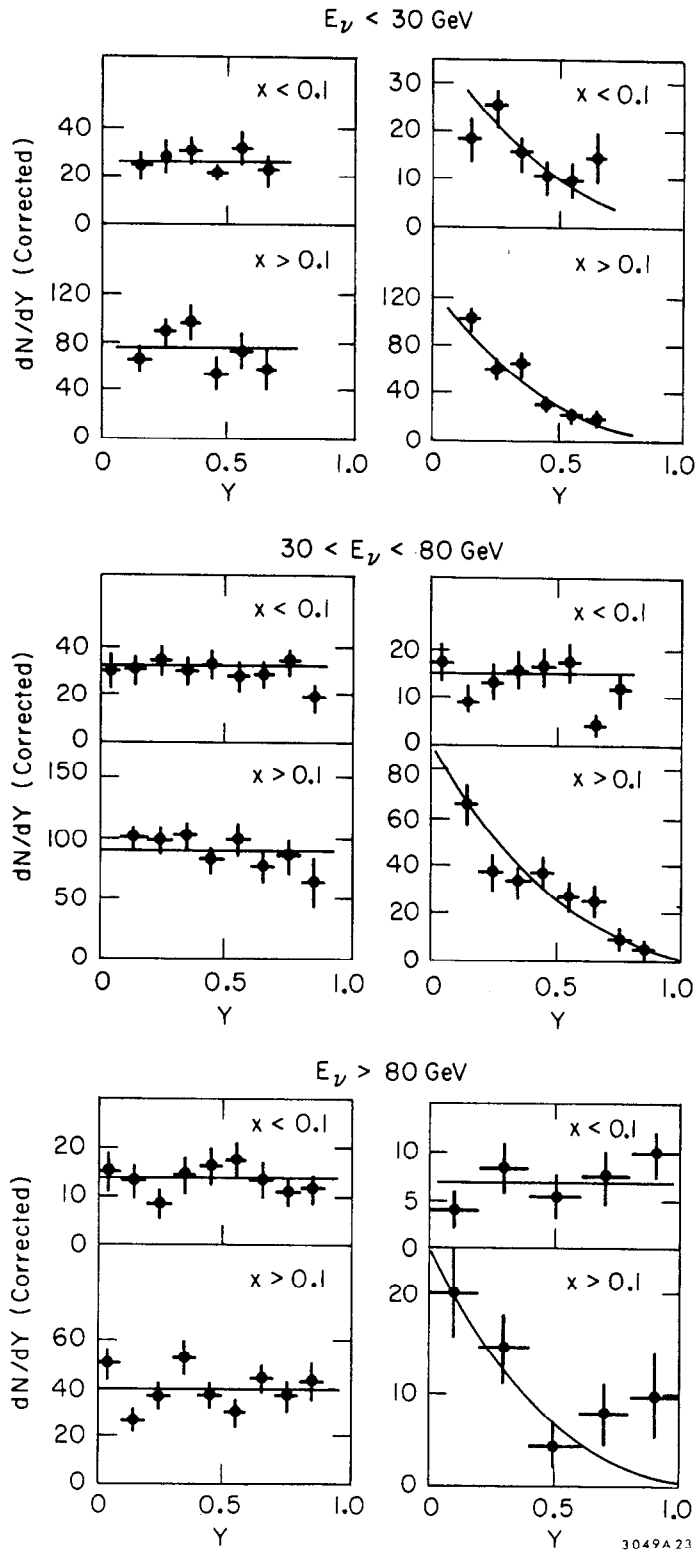


Fig. 25 y distributions for different energies from the HPWF experiment. The ν data is plotted on the left, the $\bar{\nu}$ data on the right.

in the regions where the efficiency for detection is quite high. This imposes a cut in y_{\max} on the data that increases with the increasing energy. As can be seen from Fig. 26, the low energy data ($E_{\bar{\nu}} < 30$ GeV) is consistent with $(1-y)^2$ but a significant isotropic term appears above 70 GeV.

The data have been analyzed as a function of the incident energy in terms of the average y value both for the neutrinos and antineutrinos, and then compared with the predictions expected for two different values of B . The prediction changes as a function of energy because of different acceptance for high y events as a function of energy. We can see from Fig. 27 that the neutrino data is rather insensitive to the B value but the anti-neutrino data appears to demand a decreasing value of B as a function of energy. Within these statistics at any one energy both the ν and $\bar{\nu}$ data can be fitted by the same value of B , indicating consistency at this level with the charge symmetry hypothesis.

The CITF group has recently presented⁴³⁾ the analysis of their 1974 data in terms of the x and y variables. Here also there is no external normalization since the data were taken with the fast (1 msec) spill. The qualitative conclusions are similar to those of the HPWF group, i.e. a flattening of the $\bar{\nu}$ y distribution at higher energies. More specifically, the fits to B yield $0.64^{+0.22}_{-0.26}$ for the neutrinos from π decay ($\bar{E}_{\nu} = 52$ GeV) and $0.36^{+0.30}_{-0.36}$ for the ν and $\bar{\nu}$ from K decay ($\bar{E}_{\nu} = 146$ GeV). If one normalizes the data at $y=0$ for $x > 0.1$ so that $\frac{d\sigma_{\nu}}{dy} \Big|_{y=0} = \frac{d\sigma_{\bar{\nu}}}{dy} \Big|_{y=0}$ in that region then one obtains good agreement with charge symmetry hypothesis for $x < 0.1$. It should be emphasized, however, that there is no independent verification that this hypothesis is valid.

In general one can make the following conclusions:

1. The isotropic term in $\bar{\nu}$ y distributions appears to increase with energy. This is illustrated in Fig. 28 taken from Nezrick's Aachen talk. The statistics however are quite poor and the effect relies mainly on the two high energy points.

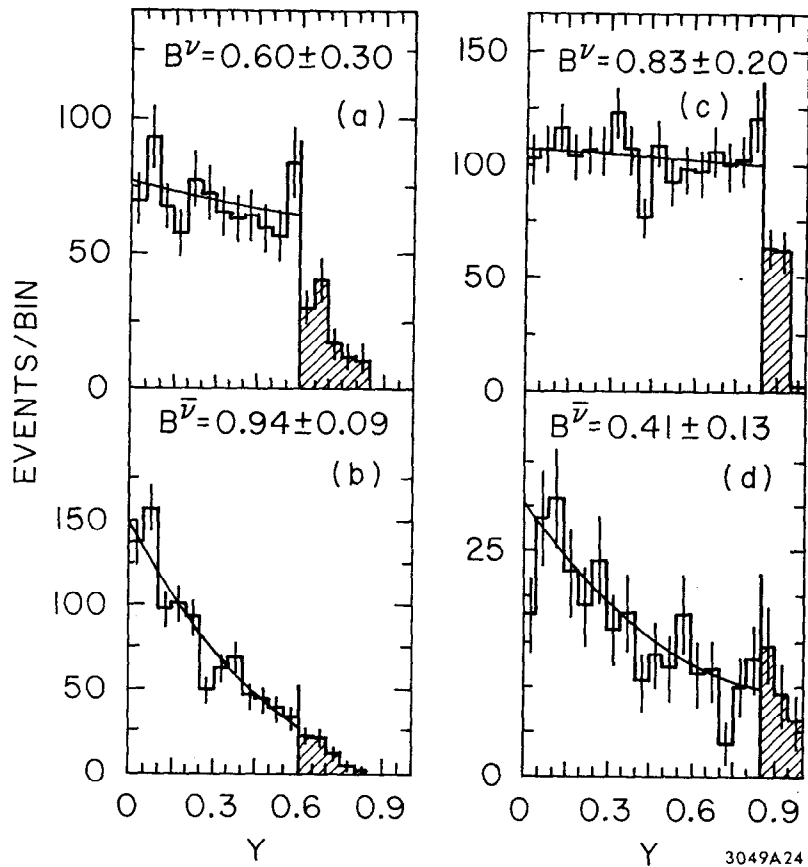
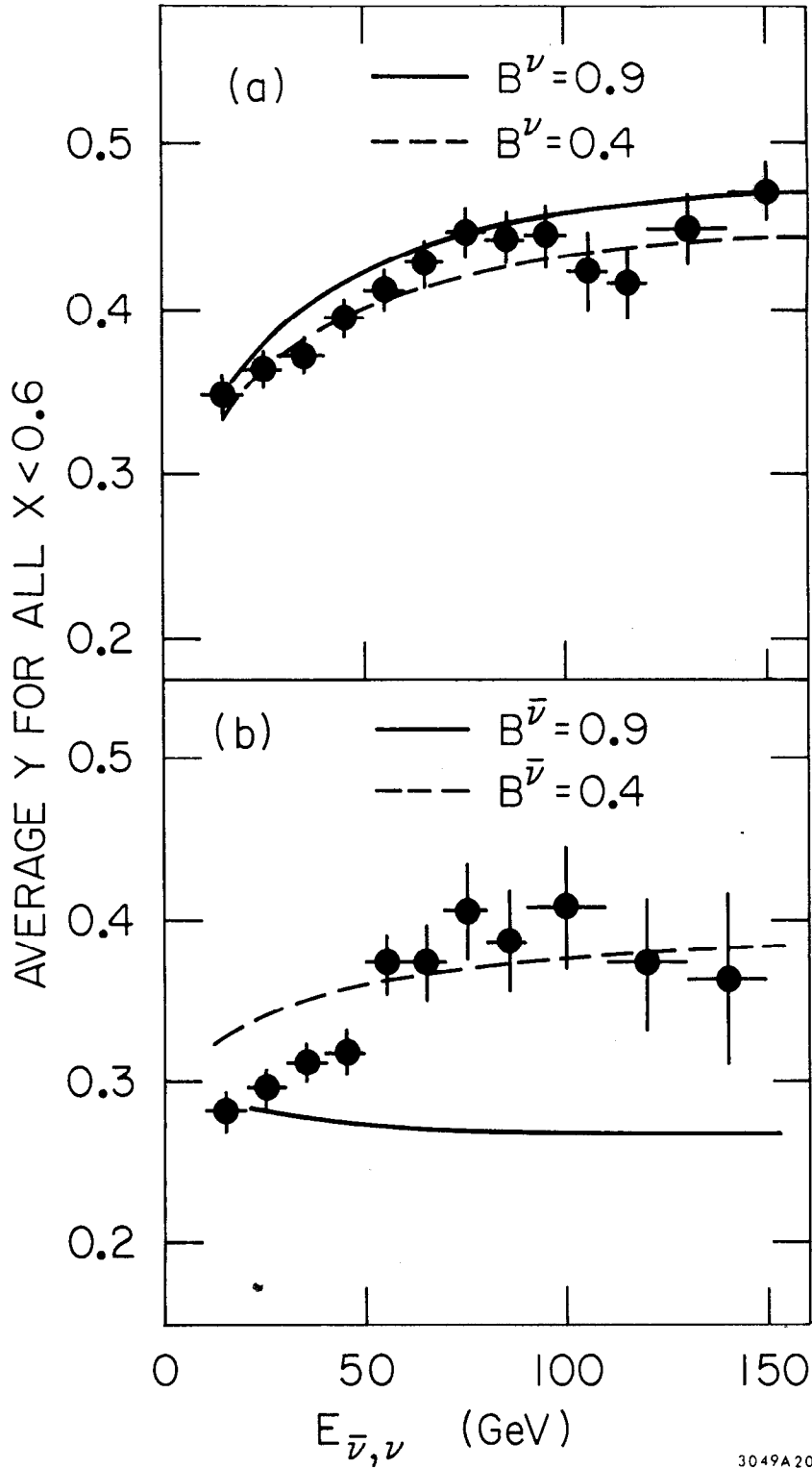


Fig. 26 The y distributions for $10 < E_{\nu} < 30$ GeV - a) for ν and b) for $\bar{\nu}$ and for $E_{\nu, \bar{\nu}} > 70$ GeV $^{2\nu}$ c) for ν and d) for $\bar{\nu}$. The cross hatched areas represent the data not used in the fit where the detection efficiency is incomplete.



3049A20

Fig. 27 Average value of y as a function of energy for the neutrino (a) and antineutrino (b) data. The expected behavior for $B_{\nu} = 0.4$ is $B_{\nu} = 0.9$ is also shown.

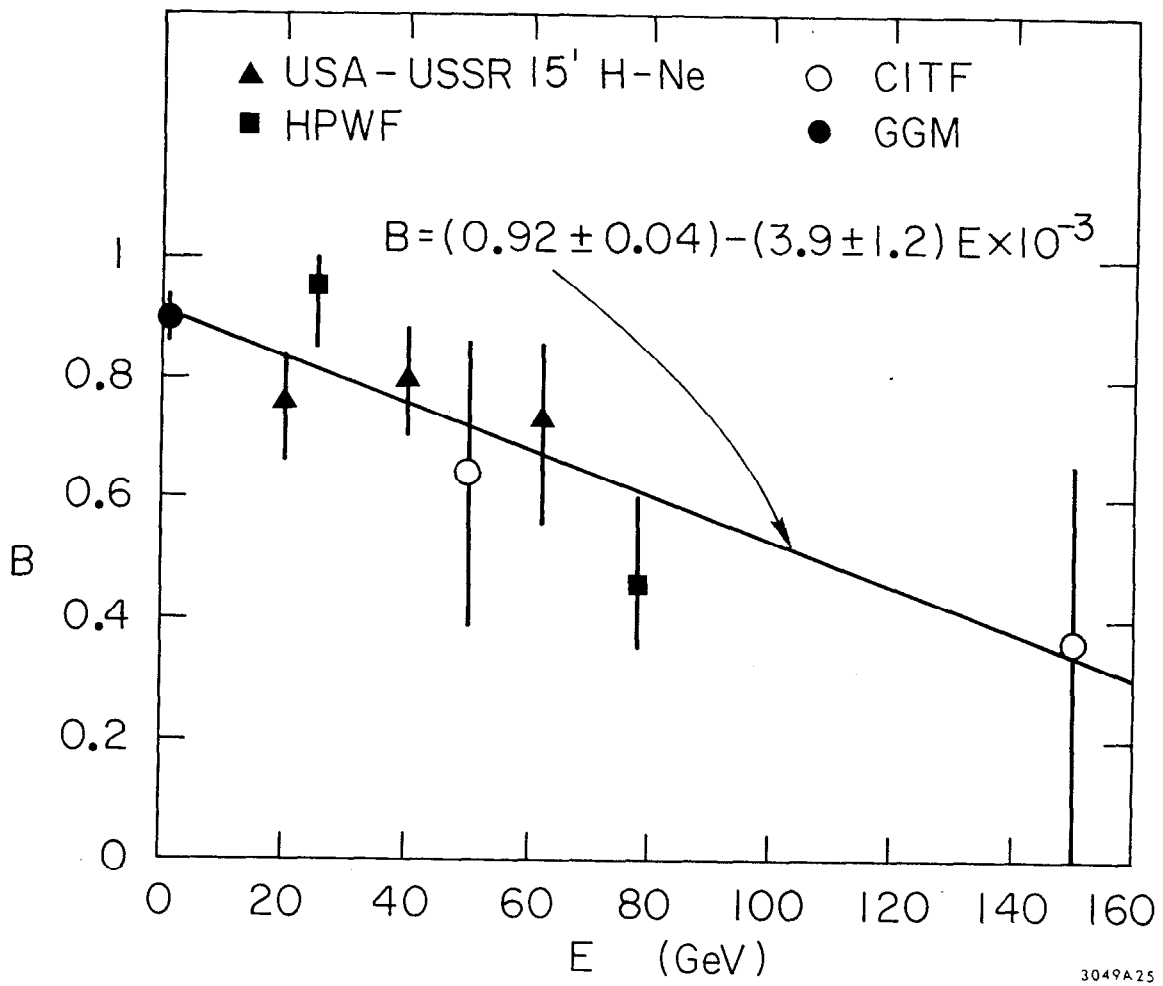


Fig. 28 A compilation of the fits to the B parameter as a function of energy.

2. There is some evidence for excess of events at low x , when compared with $F_2(x)$ obtained from ed scattering. This is probably consistent with the recent data from lepton scattering.
3. There appears to be no compelling evidence for charge symmetry violation.

VIII. $\sigma_{\text{TOTAL}} \text{ AND THE RATIO } \sigma_c(\bar{\nu})/\sigma_c(\nu)$

The question that has not been answered by the data discussed above is whether the flattening of the y distribution (so called y anomaly) represents an excess of events at high y as charge symmetry would demand or a depletion of events at low y or overall redistribution in y , both of which would imply violation of charge symmetry. The answer to that question can only come from a measurement of total ν and $\bar{\nu}$ cross sections or at least their ratio, a traditionally difficult measurement in neutrino physics.

To date, there is only one measurement of cross sections that relies on absolute flux measurement.¹³⁾ Even though rather weak statistically (it relies only on 11 $\bar{\nu}$ events at the higher energy) it appears to be consistent with no rise in the $\sigma_c(\bar{\nu})/\sigma_c(\nu)$ ratio. Specifically it yields for that ratio

$$0.40 \pm 0.11 \text{ at } 38 \text{ GeV}$$

$$\text{and } 0.23 \pm 0.11 \text{ at } 107 \text{ GeV}$$

Insofar as the detection apparatus does not see all the events because of the limited size of the magnet, one has to assume a distribution for $\frac{d\sigma}{dy}$ in order to make a correction. Assuming the form

$$\frac{d\sigma}{dy} = \alpha + (1-y)^2$$

the CITF group uses $\alpha = 0.17^{+0.3}_{-0.15}$ to calculate the total cross section from the observed events. Since $B = 1-2\alpha$, the value of α used may be low in light of the more recent results. Too low a value of α would tend to

reduce the calculated $\sigma_c(\bar{\nu})/\sigma_c(\nu)$ ratio.

If one interprets the recent CITF results⁴³⁾ on y distribution in the framework of charge symmetry validity at $y=0$ then one obtains the following numbers for the cross section ratios

$$0.52 \begin{matrix} +.15 \\ -.11 \end{matrix} \text{ at } 50 \text{ GeV}$$

and $0.69 \begin{matrix} +.31 \\ -.19 \end{matrix} \text{ at } 150 \text{ GeV}$

i.e. an apparent disagreement with the older result at the high energy.

The original measurement of the cross section ratio by the HPWF group¹⁴⁾ relied on a quadrupole focused beam and a calculation of the relative ν and $\bar{\nu}$ yield based on the yield measurements of charged π 's and K's. That result indicated no statistically significant departure from the ratio of 1/3 up to an energy of 70 GeV.

More recently much more extensive measurements have been made⁴⁴⁾ utilizing both a quadrupole focused beam and a horn focused beam. Three independent methods were used to calculate the ν and $\bar{\nu}$ flux:

1. for quadrupole beam data only, one can calculate the ν , $\bar{\nu}$ fluxes from the measured yields of π^+ , π^- , K^+ , K^- and the focusing properties of the quadrupole system. This is essentially the same method as used in the original measurement.
2. For all the data, one calculates the flux assuming the equality and energy independence of quasielastic and N^* cross sections for neutrinos and antineutrinos. This method is used here up to 60 GeV as the statistics are said to be too limited above this energy.
3. using the arguments put forth by Sakurai,⁴⁵⁾ one assumes the equality of $\frac{d\sigma}{dW^2}$ for low values of W for the neutrinos and antineutrinos. The range of values of W used is varied to check the self consistency of the method.

The three sets of measurements are displayed in Fig. 29 and they appear to yield a consistent answer, namely that the ratio of cross sections rises as the energy increases and reaches a value around 0.6 at 100 GeV.

IX. OVERALL SUMMARY

We would like to end these lectures with an overall comparison of the data with the predictions of the charm model, and specifically point out which are the questions that might present most severe difficulties for the GIM model.

We might first address ourselves to the comparison of the dilepton data and the γ anomaly, and ask whether they both could be two different manifestations of the same phenomena, i.e. the production and decay of a charmed particle. It is our feeling that the dilepton data appears quite consistent with the charm picture, except possibly for too high a rate of $\mu^+ \mu^-$ events vis a vis $\mu^- e^+$ events. The two crucial questions regarding the dilepton events are their energy dependence and the average number of strange particles associated with each event. Hopefully both of these questions will be resolved in the near future by higher statistics experiments, like the Columbia-BNL exposure in a heavy neon filled 15' bubble chamber.

Is the γ anomaly real and is it related to the dilepton events? The experimental evidence for the γ anomaly is mounting but at the same time the evidence increases for lack of the anomaly at lower energies, energies where the dilepton production appears already to be high. The HPWF group argues that both the dimuon events and the γ anomaly come in around 40 GeV, but the μe data and the recent Serbukhov results, as well as strong experimental biases against detection of 2μ events, argue, to me at least, against this hypothesis.

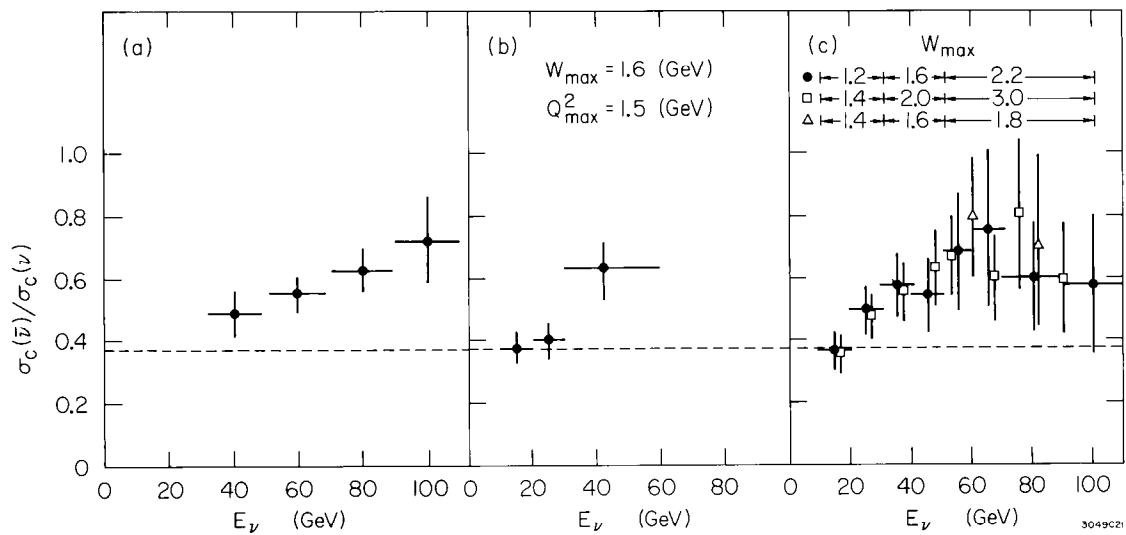


Fig. 29 $\sigma_{\bar{\nu}}/\sigma_{\nu}$ measurements by the HPWF group as a function of energy. The three different techniques for flux determination are discussed in the text.

Furthermore, the size of the y anomaly and the accompanying rise in $\bar{\nu}$ cross section, if confirmed by further experiments, appear difficult to understand in the framework of the GIM picture, since the charm contribution here is not expected to be very big. It is tempting to speculate here about these phenomena being evidence for additional quark production. A variety of models can be constructed⁴⁶⁾ which can explain the data very well if one assumes the production of a heavy quark with a mass in the 3-4 GeV range. To obtain the large y anomaly, one would have to invoke right handed coupling for the new quark.

Another approach to the explanation of the y anomaly and the rising cross section ratio assumes a scaling violation at high energy, or more specifically an increase in the $q-\bar{q}$ sea at high energy.⁴⁷⁾ To me, at least, this kind of picture appears rather unattractive and ad hoc.

In summary, we can say that in spite of the spectacular success of the GIM model in predicting the observed phenomena in e^+e^- annihilations some doubt still remains whether the GIM picture describes the whole story in neutrino interactions. The possibility of "something else" is very real and only further data will help to resolve this question.

REFERENCES

1. A. K. Mann, New Vistas in Neutrino Physics, Paper presented at the Orbis Scientiae 1976. University of Miami, Coral Gables, Florida, January, 1976.
2. For a more detailed discussion of dichromatic beams see F. Sciulli et al., Fermilab proposal E-21.
3. This scheme was used by the Cal Tech-Fermilab group in their Fermilab experiment E-262. See also proposal E-320.
4. This is the arrangement of the detector at the CERN SPS.
5. See for example L. Mo et al., Fermilab proposal E-253; also W. Lee et al., paper submitted to the 1976 Aachen Neutrino Conference.
6. R. J. Cence et al., The External Muon Identifier for the Fermilab 15-ft Bubble Chamber. LBL-4816; also submitted to Nucl. Instr. and Methods.
7. A DeRujula et al., RMP 46, 391 (1974); V. Berger and R. Phillips, Nucl. Ph. B73, 269 (1974). R. McElhaney and S. F. Tuan, Nucl. Ph. B72, 487(1974).
8. N. P. Samios, 1975 Symposium on Lepton and Photon Interactions of High Energies, Stanford, California.
9. S. J. Barish et al., ANL-HEP-PR 75-36.
10. M. Haguenaer, La Physique des Neutrino a Haute Energie, p.327, CNRS, Paris 1975.
11. G. Myatt and D. H. Perkins, Phys. Lett. 34B, 542 (1971).
12. Gargamelle collaboration, paper presented at the 1976 Tbilisi Conference.
13. B. C. Barish et al., Phys. Rev. Lett. 35, 1316 (1975).
14. A. Benvenuti et al., Phys. Rev. Lett. 32, 125 (1974).
15. For a more detailed discussion of this process see L. N. Chang et al., Phys. Rev. Lett. 35, 1252 (1975).
16. J. Blietschau et al., Phys. Lett. 60B, 207 (1976).
17. Gargamelle Collaboration, Observation of Muon-neutrino Reactions Producing a Positron and a Strange Particle, CERN/EP/PHYS 76-31.
18. W. Lee et al., a paper submitted to the June, 1976, Aachen conference.
19. J. von Krogh et al., Phys. Rev. Lett. 36, 710 (1976) and the mini-rapporteur talk by M. L. Stevenson at the 1976 Tbilisi conference, CERN/EP/PHYS 76-38.
20. J. P. Berge et al., Phys. Rev. Lett. 36, 127 (1976).

21. V. Barger and R.J.N. Phillips, Phys. Rev. Lett. 36, 1226 (1976).
22. J. P. Berge et al., Search for μe Events in Antineutrino-Nucleon Interactions, a paper submitted to the Aachen Neutrino Conference (1976).
23. C. Rubbia (HPWF collaboration), XVII International Conference on High Energy Physics, London 1974, p. IV-118.
24. A Benvenuti et al., Phys. Rev. Lett. 34, 419 (1975); A. Benvenuti et al., Phys. Rev. Lett. 35, 1199 (1975) and 35, 1203 (1975).
25. A. Benvenuti et al., Phys. Rev. Lett. 35, 1249 (1975).
26. B. C. Barish et al., Phys. Rev. Lett. 36, 939 (1976).
27. A. E. Asratyan et al., Further Search for Muonic Pairs in the neutrino and Antineutrino Beams at the IHEP 70 GeV Accelerator, paper submitted to the 1976 Aachen Conference on Neutrino Physics.
28. W. Czyz, G. C. Sheppey and J. D. Walecka, Nuovo Cimento 24, 404 (1964).
29. A. Pais and S. B. Treiman, Phys. Rev. Lett. 35, 1206 (1975).
30. S. L. Glashow, J. Iliopoulos, L. Maiani, Phys. Rev. D2, 1285 (1970).
31. M. K. Gaillard, B. W. Lee and J. L. Rosner, Rev. Mod. Phys. 47, 277 (1975).
32. S. J. Barish et al., Phys. Rev. Lett. 33, 1446 (1974).
33. H. Deden et al., Phys. Lett. 58B, 361 (1975).
34. M. Derrick et al., Phys. Rev. Lett. 36, 936 (1976).
35. J. W. Chapman et al., Phys. Rev. Lett. 36, 124 (1976).
36. E. G. Cazzoli et al., Phys. Rev. Lett. 34, 1125 (1975).
37. For an extensive discussion of various models, see A. De Rujula et al., Rev. of Mod. Ph. 46, 391 (1974).
38. J. P. Berge et al., Phys. Rev. Lett. 36, 639 (1976).
39. M. Derrick et al., Phys. Rev. Lett. 36, 936 (1976).
40. F. Nezzrick, Scaling Variable Distributions for Antineutrino-Nucleon Scattering in the 15-ft Bubble Chamber at Fermilab, Fermilab-Conf.-76/68-EXP. Paper presented at the 1976 Neutrino Conference in Aachen.
41. B. Aubert et al., Phys. Rev. Lett. 33, 984 (1974).
42. A. Benvenuti et al., Phys. Rev. Lett. 36, 1478 (1976).
43. B. C. Barish et al., Charged Current Differential Distributions in the Caltech-Fermilab ν -Experiment, CALT 68-560, paper presented at the 1976 Neutrino Conference in Aachen.

44. A Benvenuti et al., Phys. Rev. Lett. 37, 189 (1976).
45. J. J. Sakurai, UCLA preprint UCLA/73/TEP/79, 1973.
46. see for example R. M. Barnett, Phys. Rev. Lett. 36, 1163 (1976).
47. see for example S. S. Gershtein and V. N. Folomeshkin, Charge Asymmetry in Neutrino Experiments above the Charmed Particle Production Threshold, paper presented to the 1976 Tbilisi Conference.